Immunohistochemical study of morphology and distribution of CD163+ve macrophages in the normal adult equine gastrointestinal tract

Immunohistochemical study of morphology and distribution of CD163^{+ve} macrophages in the normal adult equine gastrointestinal tract

Zofia M. Lisowski[a], Kristin A. Sauter[a], Lindsey A. Waddell[a], David A. Hume[b,¥], Scott Pirie[a,¥] Neil P.H. Hudson[a,¥]

[a] The Royal (Dick) School of Veterinary Studies and The Roslin Institute, University of Edinburgh, Edinburgh, United Kingdom

[b] Mater Research Institute-University of Queensland, Woolloongabba, QLD, Australia

[¥] Joint senior co-authors

Corresponding author: Zofia Lisowski, Royal (Dick) School of Veterinary Studies and The Roslin Institute, University of Edinburgh, Edinburgh, United Kingdom Zofia.lisowski@ed.ac.uk 0131 6517300

Abstract

Intestinal macrophages are the largest group of mononuclear phagocytes in the body and play a role in intestinal innate immunity, neuroimmune interactions and maintaining intestinal homeostasis. Conversely, they also are implicated in numerous pathologies of the gastrointestinal tract, such as postoperative ileus and inflammatory bowel disease. As a result, macrophages could be potential therapeutic targets. To date, there are limited studies on the morphology and distribution of macrophages in the equine gastrointestinal tract (GIT). The aim of

this study was to identify the location and abundance of resident macrophages in the equine GIT using CD163 as an immunohistochemical marker. Tissue samples were obtained post-mortem from 14 sites along the gastrointestinal tracts of 10 horses free from gastrointestinal disease; sample sites extended from the stomach to the small colon. $CD163^{+ve}$ cells were present in all regions of the equine GIT from stomach to small colon. $CD163^{+ve}$ cells were also identified in all tissue layers of the intestinal wall; namely, mucosa, submucosa, *muscularis externa* (*ME*), myenteric plexus and serosa. Consistent with a proposed function in regulation of intestinal motility, $CD163^{+ve}$ cells were regularly distributed within the *ME*, with accumulations closely associated with the myenteric plexus and effector cells such as neurons and the interstitial cells of Cajal (ICC).

Keywords: horse; CD163; macrophage; gastrointestinal tract; intestine; inflammation

Abbreviations

BMP bone morphogenetic protein

GIT Gastrointestinal tract

ICC Interstitial cells of Cajal

LpM Lamina propria macrophages

ME *muscularis externa*

MM *muscularis* macrophages

MP myenteric plexus

POI Postoperative ileus

Introduction

Resident tissue macrophages are abundant in every organ and adapt in each location to perform tissue-specific roles. Resident intestinal macrophages are a good example of this heterogeneity. They are suitably adapted to maintain intestinal mucosal homeostasis, in addition to playing a role in infection and inflammation within what is considered a unique and difficult environment due to constant antigenic challenge from intestinal luminal contents. It is therefore unsurprising that the gastrointestinal tract (GIT) represents the largest reservoir of macrophages in the body (Lee et al., 1985). Intestinal macrophages are divided into two distinct sub-populations: lamina propria or mucosal macrophages (LpM) and *muscularis* macrophages (MM). Their survival is dependent upon signals from the macrophage colony-stimulating factor receptor (CSF1R), and in mice they are rapidly depleted by treatment with anti-CSF1R antibody (MacDonald et al., 2010). Intestinal macrophages, like most tissue macrophages, are derived from precursors from the yolk sac or fetal liver. However, LpM were shown to turn over relatively rapidly with replacement from blood monocytes in both mouse (Bain et al., 2014) and humans (Bujko et al., 2018). In comparison to LpM, MM have a slower turnover rate and are long-lived (Mikkelsen et al., 2004) although more recent studies in mice suggest the presence of a longer-lived sub-population of LpM defined by expression of the surface markers CD4 and TIM4 (Shaw et al., 2018). Long-lived MM are both embryonic and monocyte-derived with a lower turnover than LpM (De Schepper et al., 2018).

The abundant LpM population in mice and humans are $CD64^{+ve}$, MHC Class II^{hi}, $CD206^{+ve}$ and $CD163^{+ve}$. Additionally, in mice LpM are $CD11b^{+ve}$, $CD11c^{+ve}$, $CD14^{+ve}$ and $CX3CR1^{+ve}$. This is in contrast to human LpM which express low

levels of these markers but instead express CD209 (Bain and Schridde, 2018). LpM are highly phagocytic and bactericidal but exist in a state of 'hypo-responsiveness'. This anergy can be attributed to the absence of the lipopolysaccharide (LPS) receptor CD14 and the failure of LpM to produce proinflammatory cytokines like tumour necrosis factor-α (TNFα) (Smythies et al., 2005). In pigs, genes for C-type lectins including CLEC7A, CD68 and SIGLEC1 were down regulated in the GIT when compared to alveolar macrophages again supporting the expectation that intestinal macrophages tend to be hypo-responsive (Freeman et al., 2012). Additionally, macrophage production and sensing of the anti-inflammatory cytokine interleukin 10 (IL10) is essential to maintain intestinal homeostasis with rodents that are IL10 deficient developing severe colitis (Zigmond et al., 2014). The position of LpM under the epithelium enables them to be ideally situated to sample luminal contents, such as bacteria or dietary antigens, using transepithelial dendrites (Niess et al., 2005). Depletion of LpM with anti-CSF1R antibody revealed an essential function in the control of proliferation and differentiation of intestinal epithelial cells by CD169 expressing cells (Sehgal et al., 2018).

MM are considered a phenotypically distinct group from LpM (Gabanyi et al., 2016; Muller et al., 2014) but do express CD64, MHC Class II, CD206 and CD163 as LpM do (Bain and Schridde, 2018). In contrast to LpM, MM express the LPS receptor CD14, meaning they can play a role in endotoxin-mediated responses within the *muscularis* (Kalff et al., 1998b). Whilst their role in the intestine has not been as extensively studied as the LpM population, rodent derived data show that MM interact with neurons to control intestinal motility. MM produce bone morphogenetic protein 2 (BMP2) which acts on the BMP

receptor on enteric neurons. Enteric neurons produce CSF1, maintaining the MM population. This bi-directional interaction regulates the smooth muscle contractions of peristalsis (Muller et al., 2014). Although MM appear in the intestinal wall during embryonic development, their development in mice is unaffected by the absence of an enteric nervous system (Avetisyan et al., 2018).

Human and rodent studies have described intestinal macrophages in all cross-sectional regions of the intestine with a variation in their morphology dependent upon their location. In the mouse, serosal macrophages are bipolar, slender, orientated parallel to the longitudinal muscle and occasionally have bifurcated processes (Mikkelsen, 2010). Cells within the circular and longitudinal muscle layers are found between the muscular bundles and have an elongated thin shape, with those in the longitudinal muscle being less elongated compared with those within the circular muscle (Kalff et al., 1998b). Their location, morphology and CSF1 responsiveness can be visualised using Csf1r reporter transgenes in mice and rats (Hawley et al., 2018; Irvine et al., 2020; Sauter et al., 2014). Macrophages between the circular and longitudinal muscle layers, at the level of the MP (also termed Auerbach's Plexus) are stellate with multiple dendrites (Kalff et al., 1998b; Mikkelsen, 2010).

Dysregulation or activation of intestinal macrophages contributes to the pathogenesis of inflammatory bowel disease and postoperative ileus (POI) (Kalff et al., 1998a; Na et al., 2019). In mice, recruited monocytes contribute to the resolution of POI and the administration of CSF1, has therapeutic potential (Farro et al., 2017). POI in horses is a life-threatening complication of abdominal surgery (Lisowski et al., 2018) yet, despite the established influential role of

118 macrophages in the pathogenesis of POI in other species, there have been few
119 studies in the horse.

120 Studies on the distribution of macrophages in the equine GIT are limited, as is the
121 number of species-specific reagents available. This may be partly attributable to
122 limited availability of appropriate immunological markers, such as F4/80 which is
123 commonly used in mice (Hume et al., 1984). A common surface marker used in
124 multiple species, including the horse, is the macrophage scavenger receptor for
125 the haemoglobin-haptoglobin complex (CD163) which distinguishes resident
126 macrophages from recently-recruited monocytes (Chapuy et al., 2019; Sauter et
127 al., 2016; Van den Heuvel et al., 1999; Yamate et al., 2000). Previously used
128 markers for macrophage identification in the horse include the following; CD163
129 to identify laminar, intestinal (mucosal), uveal and alveolar macrophages
130 (Faleiros et al., 2011; Grosche, 2011; Karagianni et al., 2013; Sano et al., 2016;
131 Yamate et al., 2000), CD68 in monocyte-derived macrophages (MDM) and
132 various tissue macrophages including the small intestine (Fidalgo-Carvalho et al.,
133 2009; Siedek et al., 2000), MHC Class II in MDM and uveal macrophages
134 (Fidalgo-Carvalho et al., 2009; Sano et al., 2016), CD14 in monocytes, tendons,
135 alveolar and peritoneal macrophages (Chelvarajan et al., 2015; Dakin et al., 2012;
136 Karagianni et al., 2013), CD172a (Sirpα) in tendon macrophages (Dakin et al.,
137 2012), TLR4 in alveolar, peritoneal and pulmonary macrophages (Karagianni et
138 al., 2013; Singh Suri et al., 2006), CD206 in tendon macrophages (Dakin et al.,
139 2012), MAC387 (MRP-8 and MRP-14) in intestinal (mucosal) macrophages
140 (Packer et al., 2005; Steuer et al., 2018) and lysozyme in mucosal macrophages
141 (Packer et al., 2005) although both MAC387 and lysozyme are non-specific for
142 macrophages since both are also expressed by granulocytes.

Significant species-specific responses exist in macrophages. For example, in response to LPS equine bone marrow-derived macrophages do not produce nitric oxide unlike rodents which do (Young et al., 2018). Several studies have highlighted that the horse immune response is more similar to that of human than mouse (Karagianni et al., 2017; Parkinson et al., 2017). Additionally, sequence analysis of human, rodent and horse genes involved in immunity have demonstrated greater synteny between horse and human than rodent and human (Hudgens et al., 2011; Tompkins et al., 2010). The significant role in immunity that macrophages play, and the reported differences in macrophage responses that occur between species, highlights the importance of studying the cells of interest in each species and not always relying on existing data derived from other species (usually rodents). In the GIT, CD163 has been used as a marker to identify both resident and inflammatory equine intestinal macrophages (Grosche et al., 2011; Nielsen et al., 2015; Yamate et al., 2000). The context of the former study focussed on changes in macrophages in the mucosa in response to inflammation and the latter focused on the demonstration of cross-reactivity of a specific anti-CD163 antibody (clone AM-3K) between various species (humans, dogs, cats, cattle, pigs and rabbits) and no quantitation was attempted. In this present study we examine the distribution of $CD163^{+ve}$ resident macrophages in the normal equine GIT by immunohistochemistry using an anti-CD163 (Clone EdHu-1) monoclonal antibody (mAb). This will form a baseline for future studies of macrophage populations within the normal equine GIT and help to improve our understanding of the equine innate immune response in the GIT.

Methods

Animals

Ten horses (median age 17 years, range 6 - 26 years) of various breeds, were admitted to the Equine Hospital at the Royal (Dick) School of Veterinary Studies for elective euthanasia (**Table 1**). Horses were euthanased with secobarbital sodium 400mg/ml and cinchocaine hydrochloride 25mg/ml (Somulose^{TM}; Arnolds/Dechra), at a dose of 1ml/10kg bodyweight via a pre-placed intravenous catheter in the left jugular vein. None of the animals had any chronic or recent history of gastrointestinal (GI) disease and post -mortem examination confirmed the absence of any gross GI pathology. The study was approved by the University of Edinburgh School of Veterinary Medicine Ethical Review Committee.

Collection of samples from the gastrointestinal tract

Following euthanasia, an incision was made in the ventral midline to expose the abdominal cavity. The GIT was removed from the body by transecting the oesophagus at the level of the diaphragm, removing the mesenteric and body wall attachments and transecting the small colon at the junction with the rectum. Spleen and liver were removed, and the GIT placed on a clean working area. Gross contamination of blood was removed with water. Full thickness 4 cm x 4 cm sections were removed from 14 anatomical locations from the stomach to the small colon (**Table 2**) and rinsed in cold phosphate-buffered saline (PBS) (Dulbecco's Phosphate Buffered Saline; Sigma-Aldrich) prior to being trimmed into smaller segments and placed in 10% neutral buffered formalin (4% formaldehyde in neutral buffered solution) (Sigma-Aldrich). Sites were selected such that the distribution of CD163^{+ve} macrophages was representative of the

equine GIT and consistently selected from the same region. Areas with immunological activity, such as Peyer's Patches were specifically not selected.

Formalin fixed tissue paraffin embedding

Tissue samples were fixed in formalin for 24-72 hours and processed overnight using an Excelsior tissue processor (Thermo Fisher Scientific), placed in moulds and embedded in paraffin wax. Sections five-micron (5 µm) in thickness were cut, mounted on slides (Superfrost Plus, Thermo Fisher Scientific), air dried for 1 hour and incubated at 55^0 C for a further hour.

Immunohistochemistry

We elected to use the mouse anti-human mAb (Clone EDHu-1) as previous work confirmed cross reactivity to both pig (Chen et al., 2019) and cattle (Fry et al., 2016). Additional studies within our group demonstrated specific cell surface staining on equine alveolar macrophages, but not on equine bone marrow-derived macrophages by flow cytometry. These findings at protein level were as expected, as indicated by mRNA-Seq analysis (data not shown). After paraffin embedding, tissue sections were deparaffinised in xylene and rehydrated in a graded ethanol series using an automated processor (Leica Autostainer; Leica Biosystems). As a routine, all sections were stained with haematoxylin and eosin (H&E) to allow subsequent confirmation of the absence of any histopathological change indicative of pre-existing underlying pathology. Additionally, heat-mediated antigen retrieval was performed on duplicate sections by placing slides in 0.01M sodium citrate buffer (pH 6.0) in a microwaveable pressure cooker at approximately 110^o C for 20 minutes. Endogenous peroxidase activity was inhibited using 3% hydrogen peroxide (Peroxidase-blocking solution; Dako REALTM, Agilent Technologies) in methanol for 30 minutes at room temperature

(RT). Slides were incubated with 100-200 µl blocking buffer (1% normal goat serum [NGS]; Abcam, 5% bovine serum albumin (BSA); Sigma in tris-buffered saline [50 mM Tris-Cl, pH 7.6; Sigma, 150 mM NaCl; Sigma, TBS; Abcam]) for 30 minutes at RT in a humidity chamber. Primary antibody (Mouse anti-human CD163 Clone EDHu1; Bio-Rad) at a dilution of 1:200 in blocking serum was applied and slides incubated for 2 hours at RT in a humidity chamber followed by washing with blocking buffer. Secondary anti-mouse antibody was applied (ImmPRESS HRP Anti-Mouse Ig [peroxidase] Polymer Detection Kit; Vector Labs) for 15-30 minutes at RT, followed by 3,3'-diaminobenzidine (DAB) (3-solution DAB kit; Vector Labs) for 10 minutes. Slides were either dehydrated and mounted with no counterstain or counterstained with haematoxylin. Once dried, slides were scanned using a Nanozoomer (Hamamatsu Photonics) and analysed using NDP.view2 (Hamamatsu Photonics).

Quantification of cells in the equine gastrointestinal tract

Tissue sections were visualised using NDP.view2 (Hamamatsu Photonics). Tissue layers were divided into the following categories; a) mucosa which included the epithelium, lamina propria and *muscularis mucosae* (if present) b) submucosa, c) *muscularis externa* which included both the inner (circular) and outer (longitudinal) muscle, d) myenteric plexus (MP) and e) the serosa. Three areas within a 2 mm region were selected for counting for each layer; 2 mm from the left side edge, the mid-point and 2 mm from the right-side edge of the tissue section. Areas to be analysed were drawn using either the rectangle or freehand region function. All areas were inspected visually prior to counting to evaluate if sections were representative. If areas were selected that were not representative of all slides a new area was selected. Altering areas based on number of space

occupying structures e.g. blood vessels was not performed as this could lead to bias of selecting areas with higher levels of positive staining. For the mucosa, submucosa and muscle layers, a 0.5 mm^2 area was measured. For the MP and serosa, a 0.1 mm^2 area was measured. Values were either multiplied by 2 or 10 respectively, to give values per mm^2. Cells were marked manually, counted and three values for each area averaged for further analysis. See **Supplementary Figure 1** for a summary of the quantification method.

Statistical analysis

Statistical analysis was performed using GraphPad Prism 8.4.0 for Windows (GraphPad Software) and significance was assumed at $p < 0.05$. Significance in CD163 staining for each tissue layer between individual regions was determined by a Wilcoxon Signed Rank Test. Significance in CD163 staining in the different layers between grouped regions (small intestine vs large intestine) was determined using a Mann–Whitney U test. All graphs were created using GraphPad Prism 8.4.0 for Windows (GraphPad Software).

Results

Presence of macrophages in the equine GIT

Sections from 14 regions of equine GIT collected from 10 horses were stained for CD163. $CD163^{+ve}$ cells were identified in all intestinal layers (mucosa, submucosa, *muscularis* and serosa) and in all regions of the GIT (stomach to small colon).

Quantification of macrophages in the equine GIT

The distribution of cells across tissue layers was not uniform. **Figure 1** shows the number of $CD163^{+ve}$ macrophages per mm^2 of tissue in all layers and regions of the equine GIT. In the distal GIT, from the ileum to the small colon, the highest density of $CD163^{+ve}$ cells were predominantly in the submucosa. No clear trend was observed from the stomach to the distal jejunum. $CD163^{+ve}$ cells were less prevalent, but evenly distributed in the *muscularis externa* throughout the full length of the GIT. In the submucosa there was a significant difference ($p \leq 0.0001$) in $CD163^{+ve}$ cells per mm^2 between the small intestine and large intestine (**Figure 2)**. A significant increase in positive cells per mm^2 was observed between the distal jejunum to the ileum ($p \leq 0.01$) and between the distal jejunum and the remainder of the sections of the distal GIT (**Supplementary Figure 2**). By contrast, the density of $CD163^{+ve}$ cells in the mucosa was relatively consistent from stomach to small colon. However, as previously noted in humans and dogs (Hume et al., 1987; Wagner et al., 2018), $CD163^{+ve}$ macrophages in the colonic mucosa were notably concentrated towards the apical regions of villi (**Figure 3c**).

Morphology of macrophages in the equine GIT

Morphological staining characteristics at each location within the GIT are detailed below:

Mucosa

$CD163^{+ve}$ cells throughout the GIT were predominantly bipolar, each with two to three processes and were located entirely beneath the basement membrane within the lamina propria. No cells or processes were observed crossing the basement membrane and epithelial layer (**Figure 3 and 4**).

Submucosa

CD163^{+ve} macrophages were present in the submucosa of all tissue sections in the small (**Figure 5**) and large intestine (**Figure 6**). In the small intestine, submucosal macrophages were a mix of round and bipolar cells (**Figure 5**); whilst in the large intestine, they were found to be predominantly round (**Figure 6**). Macrophages were also observed adjacent to gut-associated lymphoid tissue (**Figure 7**).

***Muscularis externa*, myenteric plexus and serosa**

CD163^{+ve} equine macrophages were present in the four areas; the serosa, within the longitudinal (outer) muscle, at the level of the MP and within the circular (inner) muscle (**Figure 8**). Equine serosal macrophages were relatively regular in their distribution (**Figure 9**). As sections were examined in cross section only, most macrophages appeared bipolar and it was not possible to visualise whether cells were ramified in this view, although occasional ramified cells were observed (**Figure 10**).

Equine CD163^{+ve} macrophages were found within the *muscularis*, predominantly lying between intermuscular bundles (**Figure 11**). These cells were uniformly distributed and aligned parallel with the muscle fibres (**Figure 12**). Most cells appeared bipolar or were identified by single areas of circular positive staining, attributable to the orientation of the cross sections (**Figure 13).**

Equine CD163^{+ve} macrophages were observed in close proximity to the MP (**Figure 8**), predominantly on the periphery of the MP, although some were also observed in the centre (**Figure 14**). Positively stained cells were bipolar and stellate-shaped in this region (**Figure 15**). The macrophage density (cells per

309 mm^2) was significantly greater($p \leq 0.0001$) adjacent to the MP compared to that
310 observed within the circular and longitudinal muscle either side of the MP in both
311 the small and large intestine (**Figure 16**).

312 Discussion

313 This study aimed to identify and provide an overview of the distribution of
314 macrophages in the normal equine GIT, with a focus on the resident MMs. The
315 densities and morphologies of cells labelled with anti-CD163 are broadly similar
316 to reports of resident macrophages in other species using both CD163 and other
317 markers. In the colon of mice, once $Ly6C^{+ve}$ monocytes enter tissues, they
318 undergo a differentiation process which involves the loss of Ly6C expression and
319 upregulation of F4/80, CX3CR1, CD163, CD11c and MHC Class II. Similarly, in
320 humans, the differentiation of $CD14^{+ve}$ monocytes into intestinal macrophages
321 involves the down-regulation of CD14 and upregulation of MHC Class II and
322 CD163 (Bain et al., 2013). The expression of CD163 on human monocytes and
323 macrophages is regulated by both pro- and anti-inflammatory signals. Pro-
324 inflammatory mediators, such as LPS, TNFα and IFN-γ, suppress CD163
325 expression; whereas, anti-inflammatory signals, such as IL-10, upregulate CD163
326 expression (Buechler et al., 2000). Equine monocytes also express CD163
327 (Steinbach et al., 2005), as do equine alveolar and peritoneal macrophages
328 (Karagianni et al., 2013). Our data supports the view that CD163 is expressed by
329 populations of resident intestinal macrophages, regardless of their location in the
330 equine GIT. CD163 plays an important role in gastrointestinal homeostasis in its
331 function as a receptor for the haemoglobin-haptoglobin complex, immune sensing
332 of bacteria and by exerting an anti-inflammatory effect via an IL10 positive

feedback loop (Fabriek et al., 2009; Moestrup and Moller, 2004). Therefore, the GIT of the horse is populated with resident intestinal macrophages with an anti-inflammatory phenotype in the steady state.

As previously reported in humans and rodents, all macrophages within the mucosa were observed in accumulations below the epithelial layer within the lamina propria (Hume et al., 1983; Nagashima et al., 1996). Other studies have shown CX3CR1^{+ve} cells to sample luminal contents via processes extending through the basement membrane, between epithelial cells into the lumen in mice (Niess et al., 2005) and in dogs CD163^{+ve} cells have been shown to have transepithelial cytoplasmic processes (Wagner et al., 2018). No CD163^{+ve} cells were observed to cross the basement membrane and epithelial layer in the current study. We cannot eliminate the possibility that there are also CD163^{-ve} macrophages in the equine GIT nor can we assess whether the macrophages in the various locations display the same level of heterogeneity demonstrated in other species. This highlights the potential value of a multi-marker approach to identify of intestinal macrophage subsets. Despite the failure to identify processes crossing the epithelial layer, it is feasible that the marker selected failed to identify a subset of CD163^{-ve} macrophages. Attempts to identify such a population, for example via the detection of MHC Class II expression would be an appropriate future objective. This could help to identify CD163^{+ve} MHC Class II^{+ve} macrophage populations and CD163^{-ve} MHC Class II^{+ve} dendritic cell population in the equine GIT.

In the submucosa, a significant increase in cells per mm^2 was observed from the distal jejunum to the ileum and this trend remained consistent for the remainder of the GIT. The increase in submucosal macrophages may reflect the change in bacterial densities of the luminal contents, with a rise in bacterial density from 10^1

– 10^3 cfu/ml in the stomach to 10^{11}-10^{12} cfu/ml in the colon (O'Hara and Shanahan, 2006). Likewise, an accumulation of $CD163^{+ve}$ cells was observed to accumulate in the apical regions of the villi and not in the crypts, which may also reflect the higher antigenic load at the apex of the villus compared to the crypt. This pattern of expression has also been observed in the dog (Wagner et al., 2018).

Submucosal macrophages are thought to be a self-maintaining population of macrophages which help to support the submucosal vasculature and enteric neurons of the submucosal plexus (De Schepper et al., 2018). Although these cells reside distant to luminal signals, depletion of the submucosal macrophages results in abnormalities in the submucosal blood supply, suggesting they may play a stabilising and protective role in remodelling the submucosal vasculature in response to immune cells in the lamina propria.

As previously reported in humans (Kalff et al., 2003), equine $CD163^{+ve}$ macrophages were found within the *ME*, predominantly lying between intermuscular bundles. In rodent wholemounts, macrophages can be seen regularly and uniformly distributed throughout the *ME* with no overlap of processes (Mikkelsen et al., 2011; Phillips and Powley, 2012). In equine tissue, the MM were predominantly bipolar but only the occasional $CD163^{+ve}$ cell was observed. This apparent interspecies difference may be attributable to the relatively greater thickness of the equine *ME* and the associated difficulty in visualising the full network of cells within a single 5µm section. In comparison, it would be possible using light microscopy, to examine the full thickness of the rodent *ME* as a whole mount in future studies.

382 Between the two muscle layers (circular and longitudinal) lies the MP. The MP
383 forms part of the enteric nervous system which is involved in the control of motor
384 function, blood flow and modulates immune and endocrine functions in the
385 intestine. In rodents, the close proximity of macrophages to the MP has been
386 clearly documented (Mikkelsen, 2010; Phillips and Powley, 2012), and the
387 functional importance of this co-localisation has been demonstrated. In mice,
388 MM regulate GI motility via the production of BMP2 that acts on enteric neurons;
389 in addition this neuro-immune communication between the enteric neurons and
390 MM also stimulates tissue protective responses (Gabanyi et al., 2016; Muller et
391 al., 2014). Equine $CD163^{+ve}$ macrophages were also observed near to the MP
392 with macrophage density (cells per mm^2) greater adjacent to the MP compared to
393 within the surrounding muscle. Interstitial cells of Cajal (ICC) are also present in
394 the MP of the equine GIT and form a network of cells closely associated to the
395 smooth muscle of the intestine (Hudson et al., 1999), and are considered
396 pacemakers and mediators of neurotransmission of the GIT (Burns et al., 1996).
397 As with the neurons, macrophages in close proximity to the ICC may suggest a
398 functional relationship between them in horses as has been demonstrated in
399 rodents

400 The classification of macrophages into M1 (classical) or M2 (alternative) is
401 widely recognised as an oversimplification of the spectrum of macrophage
402 phenotypes (Hume, 2015). However, proposed M2 markers such as CD163 and
403 CD206 are considered to contribute to an overall anti-inflammatory phenotype
404 and $CD206^{+ve}$ cells are thought to contribute to resolution of inflammation in
405 inflammatory bowel disease in humans (Vos et al., 2012). In humans and rodents
406 there is heterogeneity in phenotype between LpM and MM with regards to the

expression of the LPS receptor CD14; MM express higher levels than LpM (Bujko et al., 2018). The activation of $CD14^{+ve}$ MM, such as occurs in surgical manipulation of the intestine results in the development of POI (Kalff et al., 1998a). Intestinal $CD14^{+ve}$ cells contribute to the pathogenesis of Crohns disease in humans (Kamada et al., 2008). These examples of other macrophage markers, that have been previously used in the horse highlight the potential benefits of further studying macrophage subsets in the horse. Ultimately it will further our understanding of the induction and resolution of inflammation in the GIT of the horse and help identify future therapeutic targets.

Conclusion

$CD163^{+ve}$ cells were present in all tissue layers of the equine intestine: mucosa, submucosa, *ME* and the serosa. $CD163^{+ve}$ cells were regularly distributed within the ME, with accumulations adjacent to the MP, and therefore to intestinal motility effector cells such as neurons and the ICC, supporting a potential influential role of macrophages on intestinal motility. Macrophages are not only involved in the regulation of intestinal homeostasis but are implicated in many pathologies of the GIT such as POI and inflammatory bowel disease. Future studies aimed at investigating whether POI or other diseases associated with intestinal dysmotility and inflammation are associated with alterations in the location, morphology or abundance of $CD163^{+ve}$ monocytes and macrophages changes, are therefore warranted.

Acknowledgments

The authors thank Chandra Logie and Craig Pennycook at the Royal (Dick) School of Veterinary Studies Pathology Department for their help with post-mortems. Additionally, the authors thank Emily Clark, Rachel Young, Lucas Lefevre and Sara Clohisey for their help with sample collection. Graphical abstract created with BioRender.

Funding

This work was supported by the Horserace Betting Levy Board (Grant RS253)

Authors' contributions

ZML, SP, NPHH and DAH conceptualised, designed and interpreted data in this study. ZML, KAS and LAW contributed to the acquisition of data. ZML analysed the data and compiled the manuscript. All authors contributed to, revised and approved the final manuscript.

Table 1. Horse details

	Age (years)	Sex	Breed
1	26	Gelding	Thoroughbred cross
2	21	Mare	Thoroughbred cross
3	10	Gelding	Thoroughbred
4	9	Gelding	Irish type
5	6	Gelding	Thoroughbred
6	23	Gelding	Highland Pony

7	19	Mare	Thoroughbred cross
8	15	Gelding	Thoroughbred cross
9	11	Gelding	Shire
10	21	Mare	Sports horse

444

445 **Table 2. Description of anatomical locations used for tissue collection of the**

446 **gastrointestinal tract**

447 GC = greater curvature; LC = lesser curvature

448

ID #	Location	Description of location
1	Stomach GC	Greater curvature “at the greatest curve”
2	Stomach LC	Midpoint of lesser curvature on inside of curve
3	Duodenum mid	approx. 50-75cm from pylorus
4	Jejunum proximal	Full circumferential sample and then further samples cut from anti-mesenteric aspect
5	Jejunum mid	
6	Jejunum distal	
7	Ileum mid	Ileum defined by ileocaecal fold, approx. 1m long. Midpoint ileum is midpoint of ileocaecal fold. Anti-mesenteric border.
8	Caecum mid	Sample taken 5cmaway from end of ileocaecal fold including taenial band
9	Right ventral colon mid	Midpoint over taenial band

10	Left ventral colon mid	Midpoint over taenial band
11	Pelvic flexure	At apex from the anti-mesenteric aspect
12	Left dorsal colon mid	Midpoint on outer edge
13	Right dorsal colon mid	Midpoint on outer edge over taenial band
14	Small colon	Midpoint overlying anti-mesenteric taenial band

Figure 1. Distribution of CD163^{+ve} macrophages in the equine gastrointestinal tract

Floating box plots showing maximum, minimum and median cells per mm^2 for each tissue layer (mucosa, submucosa, circular and longitudinal muscle, myenteric plexus and serosa) along the length of the equine gastrointestinal tract from (L-R); stomach lesser curvature (LC), stomach greater curvature(GC), duodenum, jejunum, ileum, caecum, right ventral colon (RVC), left ventral colon (LVC), pelvic flexure (PF), left dorsal colon (LDC), right dorsal colon (RDC) and small colon. n=10

Figure 2. Comparison between cells /mm^2 in the submucosa of the small intestine and large intestine.

Floating box plot (minimum, maximum and median) showing individual values (black dots) of cells/mm^2 in the submucosa of the small intestine (encompassiong regions from the stomach to the ileum) and the large intestine (encompassing

regions from the caecum to the small colon). Difference in cells/mm2 as measured by a Mann–Whitney U test. ****$p \leq 0.0001$

Figure 3. Lamina propria macrophages in the equine stomach, jejunum and right ventral colon

Staining for CD163 using 3,3'-diaminobenzidine (DAB) as a chromogen in the mucosa of the equine stomach (**A**), jejunum (**B**) and right ventral colon (**C**). Red line represents basement membrane. Magnification X10. Bar=250µm. Images representative of samples taken from 10 horses.

Figure 4 Morphology of lamina propria macrophages in the equine jejunum and right dorsal colon

Staining for CD163 in the lamina propria of the equine jejunum (**A**) and right dorsal colon (**B**) using 3,3'-diaminobenzidine (DAB) as a chromogen with haematoxylin as a counterstain. (**A**) is a cross section. (**B**) is a whole mount. Yellow arrow = bipolar macrophage. Green arrow = macrophages with 3 or more ramifications. (**A**) and (**B)** X20 magnification Bar=100µm. Inset X80 Bar=25µm. Images representative of samples taken from 10 horses.

Figure 5 Morphology of macrophages in the submucosa of the equine small intestine

Staining for CD163 in the submucosa of the equine jejunum (**A**) and ileum (**B**) using 3,3'-diaminobenzidine (DAB) as a chromogen with haematoxylin as a

488 counterstain. Bipolar macrophages = green arrow, blue inset. Round macrophages
489 = yellow arrow, red inset. (**A**) and (**B)** X20 magnification; Bar=100µm. Inset X80
490 Bar=25µm. Images representative of samples taken from 10 horses.

491

492 **Figure 6 Morphology of macrophages in the submucosa of equine large**
493 **intestine**

494 Staining for CD163 in the submucosa of the equine pelvic flexure (**A**) and left
495 dorsal colon (**B**) using 3,3'-diaminobenzidine (DAB) as a chromogen with
496 haematoxylin as a counterstain. Macrophages in the submucosa are predominantly
497 round (red inset) with occasional bipolar cells (blue inset).

498 (**A**) and (**B)** X20 magnification Bar=100µm. Inset X80 Bar=25µm. Images
499 representative of samples taken from 10 horses.

500

501 **Figure 7 Macrophages in gut- associated lymphoid tissues in the equine large**
502 **intestine**

503 Staining for CD163 in the equine right ventral colon using 3, 3'-diaminobenzidine
504 (DAB) as a chromogen with haematoxylin as a counterstain. (**A**) X2.5
505 magnification; Bar=1mm. Inset (**B**) X20 Bar=100µm. Images representative of
506 samples taken from 5 horses.

507

508 **Figure 8 Macrophages in the equine *muscularis externa***

Staining for CD163 in the equine duodenum using 3, 3'-diaminobenzidine (DAB) as a chromogen with haematoxylin as a counterstain. (**A**) shows a low power field of view (X5 magnifiaction) of the *muscularis externa* (ME). **CM, MP, LM** and **S** represent high power view (X 20 magnification) of circular muscle (**CM**), myenteric plexus (**MP**), longitudinal muscle (**LM**) and serosa (**S**). (A) X5 magnification Bar=500µm. (**CM, MP, LM, S**) X20 magnification Bar=100µm. Images representative of samples taken from 10 horses.

Figure 9 Serosal macrophages in the equine gastrointestinal tract

Staining for CD163 in the serosa of the equine duodenum (**A**), ileum (**B**) and caecum (**C**) using 3, 3'-diaminobenzidine (DAB) as a chromogen with haematoxylin as a counterstain. Magnification X40 magnification; Bar=50µm. Images representative of samples taken from 10 horses.

Figure 10 Ramified macrophages in the serosa of equine left ventral colon

Staining for CD163 in the serosa of equine left ventral colon using 3, 3'-diaminobenzidine (DAB) as a chromogen with haematoxylin as a counterstain. Black arrow shows macrophage with ramified morphology. Magnification X40 magnification. Bar=50µm. Image representative of samples taken from 5 horses.

Figure 11 *Muscularis* macrophages in the equine ileum

Staining for CD163 in the muscularis (circular muscle) of the equine ileum using 3, 3'-diaminobenzidine (DAB) as a chromogen with haematoxylin as a

counterstain. Macrophages were predominalty found between muscle bundles (black arrows) although occasional staining for CD163 was observed within a muscular bundle (red circle). Magnification X10. Bar=250µm. Image representative of small and large intestinal samples in 10 horses.

Figure 12 *Muscularis* macrophages in equine duodenum

Staining for CD163 in the muscularis (longitudinal layer) of the equine duodenum using 3, 3'-diaminobenzidine (DAB) as a chromogen with haematoxylin as a counterstain. Macrophages were observed between muscle bundles running longitudinally with the muscle (inset). Magnification X20. Bar=100µm. Inset X40. magnification. Bar=50µm Image representative of small and large intestinal samples in 10 horses.

Figure 13 Morphology of intermuscular *muscularis* macrophages in equine ileum

Staining for CD163 in the muscularis (circular muscle) of the equine ileum using 3, 3'-diaminobenzidine (DAB) as a chromogen with haematoxylin as a counterstain. Macrophages were predominalty bipolar (black arrows) although occasional cicular cell bodies were observed (red circle). Magnification X40. Bar=50µm. Image representative of small and large intestinal samples in 10 horses.

Figure 14 Macrophages associated with the myenteric plexus in the equine gastrointestinal tract

Staining for CD163 in the myenteric plexus (**MP**) of the equine jejunum using 3, 3'-diaminobenzidine (DAB) as a chromogen with haematoxylin as a counterstain. Macrophages were observed both on the edge of the MP (black arrows) and within the MP (red arrows). Magnification X40. Bar=50µm. CM, cricular muscle. LM, longitudinal muscle. Image representative of small and large intestinal samples in 10 horses.

Figure 15 Morphology of myenteric plexus macrophages in the equine gastrointestinal tract

Staining for CD163 in the myenteric plexus of the equine jejunum using 3, 3'-diaminobenzidine (DAB) as a chromogen with haematoxylin as a counterstain. The morphology of myenteric plexus macrophages was either round (**A**) or ramified (**B**). Magnification X80. Bar=25µm. Image representative of small and large intestinal samples in 10 horses.

Figure 16 Comparison of cells/mm2 between the *muscularis externa* and myenteric plexus of the small and large intestine.

Floating box plot (minimum, maximum and median) showing individual values (black dots) of cells/mm^2 in the *muscularis externa* (circular muscle and longitudinal muscle) of the small intestine and the large intestine. Difference in cells/mm^2 as measured by a Mann–Whitney U test. Significance = ****$p \leq 0.000$.

Avetisyan, M., Rood, J.E., Huerta Lopez, S., Sengupta, R., Wright-Jin, E., Dougherty, J.D., Behrens, E.M., Heuckeroth, R.O., 2018. Muscularis macrophage development in the absence of an enteric nervous system. Proc Natl Acad Sci U S A 115, 4696-4701.

Bain, C.C., Bravo-Blas, A., Scott, C.L., Perdiguero, E.G., Geissmann, F., Henri, S., Malissen, B., Osborne, L.C., Artis, D., Mowat, A.M., 2014. Constant replenishment from circulating monocytes maintains the macrophage pool in the intestine of adult mice. Nat Immunol 15, 929-937.

Bain, C.C., Schridde, A., 2018. Origin, Differentiation, and Function of Intestinal Macrophages. Frontiers in immunology 9, 2733.

Bain, C.C., Scott, C.L., Uronen-Hansson, H., Gudjonsson, S., Jansson, O., Grip, O., Guilliams, M., Malissen, B., Agace, W.W., Mowat, A.M., 2013. Resident and pro-inflammatory macrophages in the colon represent alternative context-dependent fates of the same Ly6Chi monocyte precursors. Mucosal Immunol 6, 498-510.

Buechler, C., Ritter, M., Orso, E., Langmann, T., Klucken, J., Schmitz, G., 2000. Regulation of scavenger receptor CD163 expression in human monocytes and macrophages by pro- and antiinflammatory stimuli. Journal of leukocyte biology 67, 97-103.

Bujko, A., Atlasy, N., Landsverk, O.J.B., Richter, L., Yaqub, S., Horneland, R., Oyen, O., Aandahl, E.M., Aabakken, L., Stunnenberg, H.G., Baekkevold, E.S., Jahnsen, F.L., 2018. Transcriptional and functional profiling defines human small intestinal macrophage subsets. The Journal of experimental medicine 215, 441-458.

Burns, A.J., Lomax, A.E., Torihashi, S., Sanders, K.M., Ward, S.M., 1996. Interstitial cells of Cajal mediate inhibitory neurotransmission in the stomach. Proc Natl Acad Sci U S A 93, 12008-12013.

Chapuy, L., Bsat, M., Sarkizova, S., Rubio, M., Therrien, A., Wassef, E., Bouin, M., Orlicka, K., Weber, A., Hacohen, N., Villani, A.C., Sarfati, M., 2019. Two distinct colonic CD14(+) subsets characterized by single-cell RNA profiling in Crohn's disease. Mucosal Immunol 12, 703-719.

Chelvarajan, R.L., Mondal, S.P., Cook, R.F., Go, Y., Sarkar, S., Henney, P., Marti, F., Bailey, E., Balasuriya, U., 2015. CD14^{hi} equine monocytes are preferential initial targets for infection with equine arteritis virus (IRC4P.615). The Journal of Immunology 194, 57.32-57.32.

Chen, J., Wang, H., Bai, J., Liu, W., Liu, X., Yu, D., Feng, T., Sun, Z., Zhang, L., Ma, L., Hu, Y., Zou, Y., Tan, T., Zhong, J., Hu, M., Bai, X., Pan, D., Xing, Y., Zhao, Y., Tian, K., Hu, X., Li, N., 2019. Generation of Pigs Resistant to Highly Pathogenic-Porcine Reproductive and Respiratory Syndrome Virus through Gene Editing of CD163. International journal of biological sciences 15, 481-492.

Dakin, S.G., Werling, D., Hibbert, A., Abayasekara, D.R.E., Young, N.J., Smith, R.K.W., Dudhia, J., 2012. Macrophage Sub-Populations and the Lipoxin A4 Receptor Implicate Active Inflammation during Equine Tendon Repair. PLOS ONE 7, e32333.

De Schepper, S., Verheijden, S., Aguilera-Lizarraga, J., Viola, M.F., Boesmans, W., Stakenborg, N., Voytyuk, I., Schmidt, I., Boeckx, B., Dierckx de Casterle, I., Baekelandt, V., Gonzalez Dominguez, E., Mack, M., Depoortere, I., De Strooper, B., Sprangers, B., Himmelreich, U., Soenen, S., Guilliams, M., Vanden Berghe, P., Jones, E., Lambrechts, D.,

627 Boeckxstaens, G., 2018. Self-Maintaining Gut Macrophages Are Essential
628 for Intestinal Homeostasis. Cell 175, 400-415.e413.
629 Fabriek, B.O., van Bruggen, R., Deng, D.M., Ligtenberg, A.J., Nazmi, K.,
630 Schornagel, K., Vloet, R.P., Dijkstra, C.D., van den Berg, T.K., 2009. The
631 macrophage scavenger receptor CD163 functions as an innate immune
632 sensor for bacteria. Blood 113, 887-892.
633 Faleiros, R.R., Johnson, P.J., Nuovo, G.J., Messer, N.T., Black, S.J., Belknap,
634 J.K., 2011. Laminar leukocyte accumulation in horses with carbohydrate
635 overload-induced laminitis. Journal of veterinary internal medicine 25,
636 107-115.
637 Farro, G., Stakenborg, M., Gomez-Pinilla, P.J., Labeeuw, E., Goverse, G., Di
638 Giovangiulio, M., Stakenborg, N., Meroni, E., D'Errico, F., Elkrim, Y.,
639 Laoui, D., Lisowski, Z.M., Sauter, K.A., Hume, D.A., Van Ginderachter,
640 J.A., Boeckxstaens, G.E., Matteoli, G., 2017. CCR2-dependent monocyte-
641 derived macrophages resolve inflammation and restore gut motility in
642 postoperative ileus. Gut 66, 2098-2109.
643 Fidalgo-Carvalho, I., Craigo, J.K., Barnes, S., Costa-Ramos, C., Montelaro, R.C.,
644 2009. Characterization of an equine macrophage cell line: application to
645 studies of EIAV infection. Vet Microbiol 136, 8-19.
646 Freeman, T.C., Ivens, A., Baillie, J.K., Beraldi, D., Barnett, M.W., Dorward, D.,
647 Downing, A., Fairbairn, L., Kapetanovic, R., Raza, S., Tomoiu, A.,
648 Alberio, R., Wu, C., Su, A.I., Summers, K.M., Tuggle, C.K., Archibald,
649 A.L., Hume, D.A., 2012. A gene expression atlas of the domestic pig.
650 BMC Biol 10, 90.
651 Fry, L.M., Schneider, D.A., Frevert, C.W., Nelson, D.D., Morrison, W.I.,
652 Knowles, D.P., 2016. East Coast Fever Caused by Theileria parva Is
653 Characterized by Macrophage Activation Associated with Vasculitis and
654 Respiratory Failure. PLoS One 11, e0156004.
655 Gabanyi, I., Muller, P.A., Feighery, L., Oliveira, T.Y., Costa-Pinto, F.A., Mucida,
656 D., 2016. Neuro-immune Interactions Drive Tissue Programming in
657 Intestinal Macrophages. Cell 164, 378-391.
658 Grosche, A., 2011. Large colon ischemia and reperfusion in horses: Histological
659 and functional alterations, and response of the innate immune system.
660 Ph.D. University of Florida, Ann Arbor.
661 Grosche, A., Morton, A.J., Graham, A.S., Valentine, J.F., Abbott, J.R., Polyak,
662 M.M., Freeman, D.E., 2011. Mucosal injury and inflammatory cells in
663 response to brief ischaemia and reperfusion in the equine large colon.
664 Equine Vet J Suppl 43, 16-25.
665 Hawley, C.A., Rojo, R., Raper, A., Sauter, K.A., Lisowski, Z.M., Grabert, K.,
666 Bain, C.C., Davis, G.M., Louwe, P.A., Ostrowski, M.C., Hume, D.A.,
667 Pridans, C., Jenkins, S.J., 2018. Csf1r-mApple Transgene Expression and
668 Ligand Binding In Vivo Reveal Dynamics of CSF1R Expression within
669 the Mononuclear Phagocyte System. J Immunol 200, 2209-2223.
670 Hudgens, E., Tompkins, D., Boyd, P., Lunney, J.K., Horohov, D., Baldwin, C.L.,
671 2011. Expressed gene sequence of the IFNgamma-response chemokine
672 CXCL9 of cattle, horses, and swine. Veterinary immunology and
673 immunopathology 141, 317-321.
674 Hudson, N.P., Pearson, G.T., Kitamura, N., Mayhew, I.G., 1999. An
675 immunohistochemical study of interstitial cells of Cajal (ICC) in the
676 equine gastrointestinal tract. Research in veterinary science 66, 265-271.

677 Hume, D.A., 2015. The Many Alternative Faces of Macrophage Activation.
678 Frontiers in immunology 6, 370.
679 Hume, D.A., Allan, W., Hogan, P.G., Doe, W.F., 1987. Immunohistochemical
680 characterisation of macrophages in human liver and gastrointestinal tract:
681 expression of CD4, HLA-DR, OKM1, and the mature macrophage marker
682 25F9 in normal and diseased tissue. Journal of leukocyte biology 42, 474-
683 484.
684 Hume, D.A., Loutit, J.F., Gordon, S., Hume, D.A., Loutit, J.F., Gordon, S., 1984.
685 The mononuclear phagocyte system of the mouse defined by
686 immunohistochemical localization of antigen F4/80. macrophages of bone
687 and associated connective tissue 66, 189-194.
688 Hume, D.A., Robinson, A.P., MacPherson, G.G., Gordon, S., 1983. The
689 mononuclear phagocyte system of the mouse defined by
690 immunohistochemical localization of antigen F4/80. Relationship between
691 macrophages, Langerhans cells, reticular cells, and dendritic cells in
692 lymphoid and hematopoietic organs. The Journal of experimental
693 medicine 158, 1522-1536.
694 Irvine, K.M., Caruso, M., Cestari, M.F., Davis, G.M., Keshvari, S., Sehgal, A.,
695 Pridans, C., Hume, D.A., 2020. Analysis of the impact of CSF-1
696 administration in adult rats using a novel Csf1r-mApple reporter gene.
697 Journal of leukocyte biology 107, 221-235.
698 Kalff, J.C., Schraut, W.H., Simmons, R.L., Bauer, A.J., 1998a. Surgical
699 manipulation of the gut elicits an intestinal muscularis inflammatory
700 response resulting in postsurgical ileus. Ann Surg 228, 652-663.
701 Kalff, J.C., Schwarz, N.T., Walgenbach, K.J., Schraut, W.H., Bauer, A.J., 1998b.
702 Leukocytes of the intestinal muscularis: their phenotype and isolation.
703 Journal of leukocyte biology 63, 683-691.
704 Kalff, J.C., Turler, A., Schwarz, N.T., Schraut, W.H., Lee, K.K., Tweardy, D.J.,
705 Billiar, T.R., Simmons, R.L., Bauer, A.J., 2003. Intra-abdominal activation
706 of a local inflammatory response within the human muscularis externa
707 during laparotomy. Ann Surg 237, 301-315.
708 Kamada, N., Hisamatsu, T., Okamoto, S., Chinen, H., Kobayashi, T., Sato, T.,
709 Sakuraba, A., Kitazume, M.T., Sugita, A., Koganei, K., Akagawa, K.S.,
710 Hibi, T., 2008. Unique CD14 intestinal macrophages contribute to the
711 pathogenesis of Crohn disease via IL-23/IFN-gamma axis. The Journal of
712 clinical investigation 118, 2269-2280.
713 Karagianni, A.E., Kapetanovic, R., McGorum, B.C., Hume, D.A., Pirie, S.R.,
714 2013. The equine alveolar macrophage: functional and phenotypic
715 comparisons with peritoneal macrophages. Veterinary immunology and
716 immunopathology 155, 219-228.
717 Karagianni, A.E., Kapetanovic, R., Summers, K.M., McGorum, B.C., Hume,
718 D.A., Pirie, R.S., 2017. Comparative transcriptome analysis of equine
719 alveolar macrophages. Equine Vet J 49, 375-382.
720 Lee, S.H., Starkey, P.M., Gordon, S., 1985. Quantitative analysis of total
721 macrophage content in adult mouse tissues. Immunochemical studies with
722 monoclonal antibody F4/80. The Journal of experimental medicine 161,
723 475-489.
724 Lisowski, Z.M., Pirie, R.S., Blikslager, A.T., Lefebvre, D., Hume, D.A., Hudson,
725 N.P.H., 2018. An update on equine post-operative ileus: Definitions,
726 pathophysiology and management. Equine Vet J 50, 292-303.

MacDonald, K.P.A., Palmer, J.S., Cronau, S., Seppanen, E., Olver, S., Raffelt, N.C., Kuns, R., Pettit, A.R., Clouston, A., Wainwright, B., Branstetter, D., Smith, J., Paxton, R.J., Cerretti, D.P., Bonham, L., Hill, G.R., Hume, D.A., 2010. An antibody against the colony-stimulating factor 1 receptor depletes the resident subset of monocytes and tissue- and tumor-associated macrophages but does not inhibit inflammation, Vol 116, 3955-3963 pp.

Mikkelsen, H.B., 2010. Interstitial cells of Cajal, macrophages and mast cells in the gut musculature: morphology, distribution, spatial and possible functional interactions. J Cell Mol Med 14, 818-832.

Mikkelsen, H.B., Garbarsch, C., Tranum-Jensen, J., Thuneberg, L., 2004. Macrophages in the small intestinal muscularis externa of embryos, newborn and adult germ-free mice. Journal of molecular histology 35, 377-387.

Mikkelsen, H.B., Larsen, J.O., Froh, P., Nguyen, T.H., 2011. Quantitative assessment of macrophages in the muscularis externa of mouse intestines. Anat Rec (Hoboken) 294, 1557-1565.

Moestrup, S.K., Moller, H.J., 2004. CD163: a regulated hemoglobin scavenger receptor with a role in the anti-inflammatory response. Annals of medicine 36, 347-354.

Muller, P.A., Koscso, B., Rajani, G.M., Stevanovic, K., Berres, M.L., Hashimoto, D., Mortha, A., Leboeuf, M., Li, X.M., Mucida, D., Stanley, E.R., Dahan, S., Margolis, K.G., Gershon, M.D., Merad, M., Bogunovic, M., 2014. Crosstalk between muscularis macrophages and enteric neurons regulates gastrointestinal motility. Cell 158, 300-313.

Na, Y.R., Stakenborg, M., Seok, S.H., Matteoli, G., 2019. Macrophages in intestinal inflammation and resolution: a potential therapeutic target in IBD. Nature Reviews Gastroenterology & Hepatology 16, 531-543.

Nagashima, R., Maeda, K., Imai, Y., Takahashi, T., 1996. Lamina propria macrophages in the human gastrointestinal mucosa: their distribution, immunohistological phenotype, and function. J Histochem Cytochem 44, 721-731.

Nielsen, M.K., Loynachan, A.T., Jacobsen, S., Stewart, J.C., Reinemeyer, C.R., Horohov, D.W., 2015. Local and systemic inflammatory and immunologic reactions to cyathostomin larvicidal therapy in horses. Veterinary immunology and immunopathology 168, 203-210.

Niess, J.H., Brand, S., Gu, X., Landsman, L., Jung, S., McCormick, B.A., Vyas, J.M., Boes, M., Ploegh, H.L., Fox, J.G., Littman, D.R., Reinecker, H.C., 2005. CX3CR1-mediated dendritic cell access to the intestinal lumen and bacterial clearance. Science (New York, N.Y.) 307, 254-258.

O'Hara, A.M., Shanahan, F., 2006. The gut flora as a forgotten organ. EMBO Rep 7, 688-693.

Packer, M., Patterson-Kane, J.C., Smith, K.C., Durham, A.E., 2005. Quantification of immune cell populations in the lamina propria of equine jejunal biopsy specimens. J Comp Pathol 132, 90-95.

Parkinson, N.J., Buechner-Maxwell, V.A., Witonsky, S.G., Pleasant, R.S., Werre, S.R., Ahmed, S.A., 2017. Characterization of basal and lipopolysaccharide-induced microRNA expression in equine peripheral blood mononuclear cells using Next-Generation Sequencing. PLoS One 12, e0177664.

776 Phillips, R.J., Powley, T.L., 2012. Macrophages associated with the intrinsic and
777 extrinsic autonomic innervation of the rat gastrointestinal tract. Auton
778 Neurosci 169, 12-27.
779 Sano, Y., Matsuda, K., Okamoto, M., Takehana, K., Hirayama, K., Taniyama, H.,
780 2016. Distribution of CD163-positive cell and MHC class II-positive cell
781 in the normal equine uveal tract. J Vet Med Sci 78, 287-291.
782 Sauter, K.A., Pridans, C., Sehgal, A., Bain, C.C., Scott, C., Moffat, L., Rojo, R.,
783 Stutchfield, B.M., Davies, C.L., Donaldson, D.S., Renault, K., McColl,
784 B.W., Mowat, A.M., Serrels, A., Frame, M.C., Mabbott, N.A., Hume,
785 D.A., 2014. The MacBlue binary transgene (csf1r-gal4VP16/UAS-ECFP)
786 provides a novel marker for visualisation of subsets of monocytes,
787 macrophages and dendritic cells and responsiveness to CSF1
788 administration. PLoS One 9, e105429.
789 Sauter, K.A., Waddell, L.A., Lisowski, Z.M., Young, R., Lefevre, L., Davis,
790 G.M., Clohisey, S.M., McCulloch, M., Magowan, E., Mabbott, N.A.,
791 Summers, K.M., Hume, D.A., 2016. Macrophage colony-stimulating
792 factor (CSF1) controls monocyte production and maturation and the
793 steady-state size of the liver in pigs. American journal of physiology.
794 Gastrointestinal and liver physiology 311, G533-547.
795 Sehgal, A., Donaldson, D.S., Pridans, C., Sauter, K.A., Hume, D.A., Mabbott,
796 N.A., 2018. The role of CSF1R-dependent macrophages in control of the
797 intestinal stem-cell niche. Nat Commun 9, 1272.
798 Shaw, T.N., Houston, S.A., Wemyss, K., Bridgeman, H.M., Barbera, T.A.,
799 Zangerle-Murray, T., Strangward, P., Ridley, A.J.L., Wang, P.,
800 Tamoutounour, S., Allen, J.E., Konkel, J.E., Grainger, J.R., 2018. Tissue-
801 resident macrophages in the intestine are long lived and defined by Tim-4
802 and CD4 expression. The Journal of experimental medicine 215, 1507-
803 1518.
804 Siedek, E.M., Honnah-Symns, N., Fincham, S.C., Mayall, S., Hamblin, A.S.,
805 2000. Equine macrophage identification with an antibody (Ki-M6) to
806 human CD68 and a new monoclonal antibody (JB10). J Comp Pathol 122,
807 145-154.
808 Singh Suri, S., Janardhan, K.S., Parbhakar, O., Caldwell, S., Appleyard, G.,
809 Singh, B., 2006. Expression of toll-like receptor 4 and 2 in horse lungs.
810 Vet Res 37, 541-551.
811 Smythies, L.E., Sellers, M., Clements, R.H., Mosteller-Barnum, M., Meng, G.,
812 Benjamin, W.H., Orenstein, J.M., Smith, P.D., 2005. Human intestinal
813 macrophages display profound inflammatory anergy despite avid
814 phagocytic and bacteriocidal activity. J Clin Invest 115, 66-75.
815 Steinbach, F., Stark, R., Ibrahim, S., Gawad, E.A., Ludwig, H., Walter, J.,
816 Commandeur, U., Mauel, S., 2005. Molecular cloning and characterization
817 of markers and cytokines for equid myeloid cells. Veterinary immunology
818 and immunopathology 108, 227-236.
819 Steuer, A.E., Loynachan, A.T., Nielsen, M.K., 2018. Evaluation of the mucosal
820 inflammatory responses to equine cyathostomins in response to
821 anthelmintic treatment. Veterinary immunology and immunopathology
822 199, 1-7.
823 Tompkins, D., Hudgens, E., Horohov, D., Baldwin, C.L., 2010. Expressed gene
824 sequences of the equine cytokines interleukin-17 and interleukin-23.
825 Veterinary immunology and immunopathology 133, 309-313.

Van den Heuvel, M.M., Tensen, C.P., van As, J.H., Van den Berg, T.K., Fluitsma, D.M., Dijkstra, C.D., Dopp, E.A., Droste, A., Van Gaalen, F.A., Sorg, C., Hogger, P., Beelen, R.H., 1999. Regulation of CD 163 on human macrophages: cross-linking of CD163 induces signaling and activation. Journal of leukocyte biology 66, 858-866.

Vos, A.C., Wildenberg, M.E., Arijs, I., Duijvestein, M., Verhaar, A.P., de Hertogh, G., Vermeire, S., Rutgeerts, P., van den Brink, G.R., Hommes, D.W., 2012. Regulatory macrophages induced by infliximab are involved in healing in vivo and in vitro. Inflammatory bowel diseases 18, 401-408.

Wagner, A., Junginger, J., Lemensieck, F., Hewicker-Trautwein, M., 2018. Immunohistochemical characterization of gastrointestinal macrophages/phagocytes in dogs with inflammatory bowel disease (IBD) and non-IBD dogs. Veterinary immunology and immunopathology 197, 49-57.

Yamate, J., Yoshida, H., Tsukamoto, Y., Ide, M., Kuwamura, M., Ohashi, F., Miyamoto, T., Kotani, T., Sakuma, S., Takeya, M., 2000. Distribution of cells immunopositive for AM-3K, a novel monoclonal antibody recognizing human macrophages, in normal and diseased tissues of dogs, cats, horses, cattle, pigs, and rabbits. Veterinary pathology 37, 168-176.

Young, R., Bush, S.J., Lefevre, L., McCulloch, M.E.B., Lisowski, Z.M., Muriuki, C., Waddell, L.A., Sauter, K.A., Pridans, C., Clark, E.L., Hume, D.A., 2018. Species-Specific Transcriptional Regulation of Genes Involved in Nitric Oxide Production and Arginine Metabolism in Macrophages. Immunohorizons 2, 27-37.

Zigmond, E., Bernshtein, B., Friedlander, G., Walker, C.R., Yona, S., Kim, K.W., Brenner, O., Krauthgamer, R., Varol, C., Muller, W., Jung, S., 2014. Macrophage-restricted interleukin-10 receptor deficiency, but not IL-10 deficiency, causes severe spontaneous colitis. Immunity 40, 720-733.

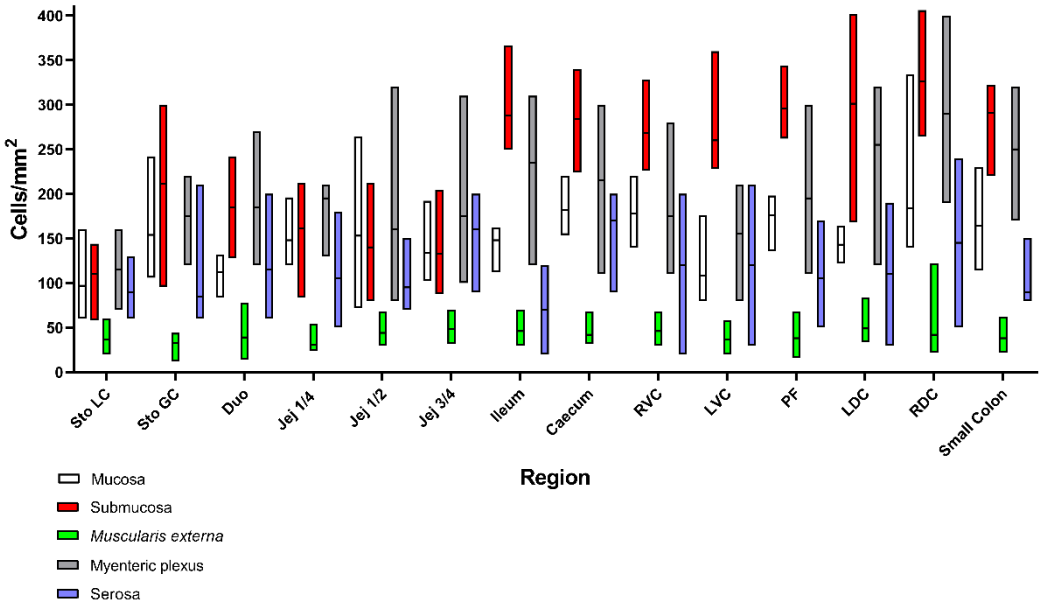

863

864 **Figure 1**

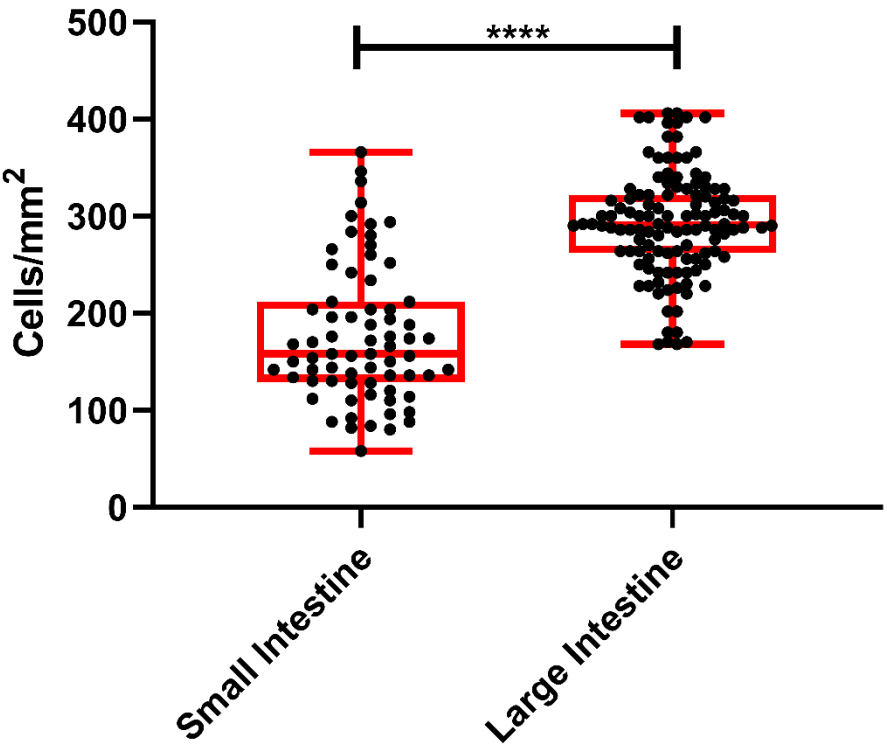

865

866 **Figure 2**

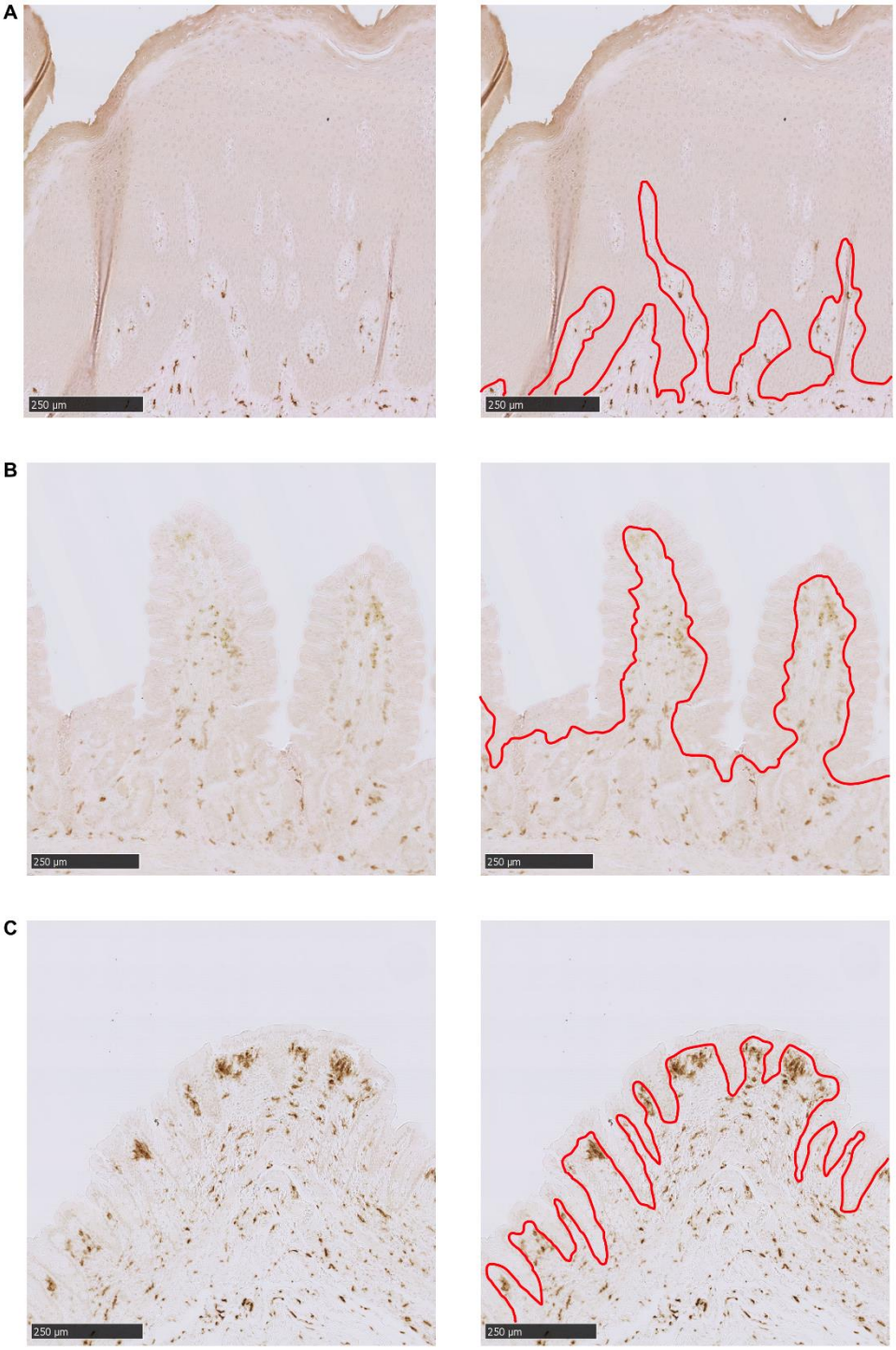

867

868 **Figure 3**

869

870

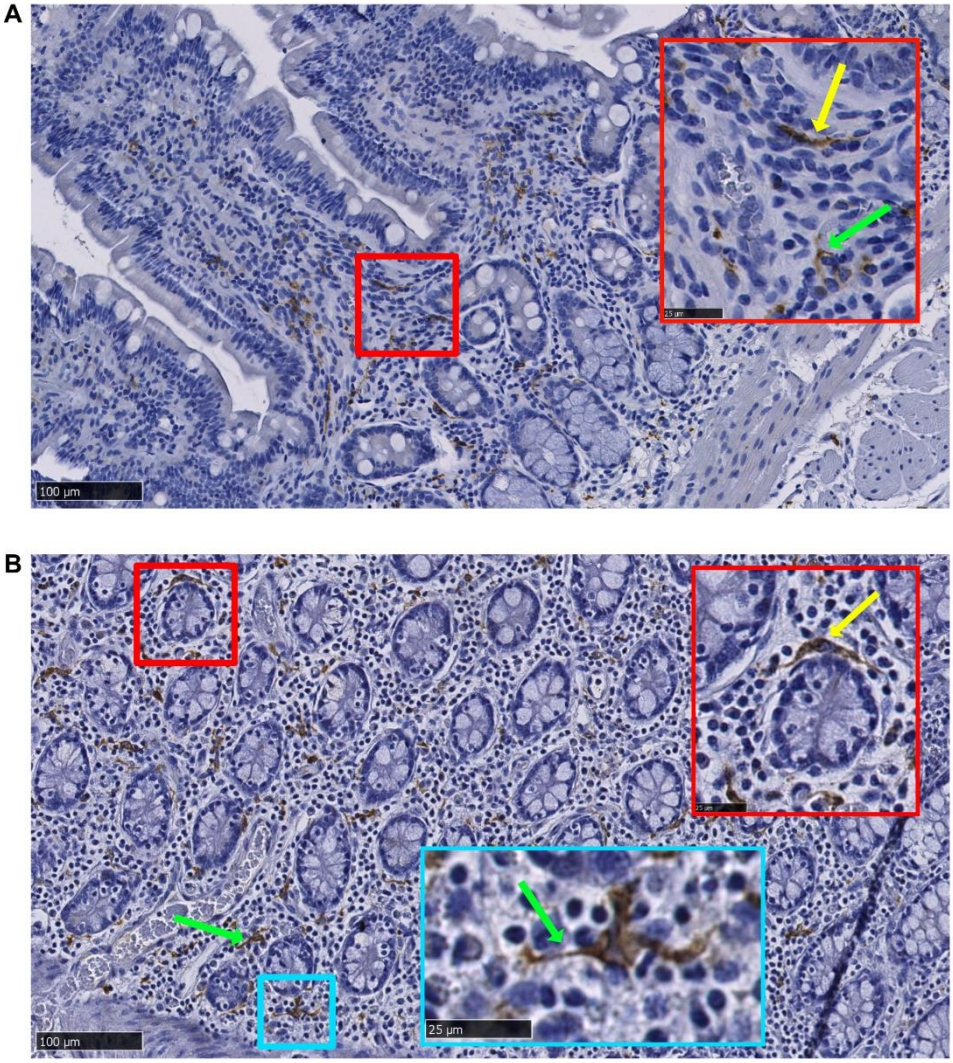

871

872 **Figure 4**

873 **Figure**

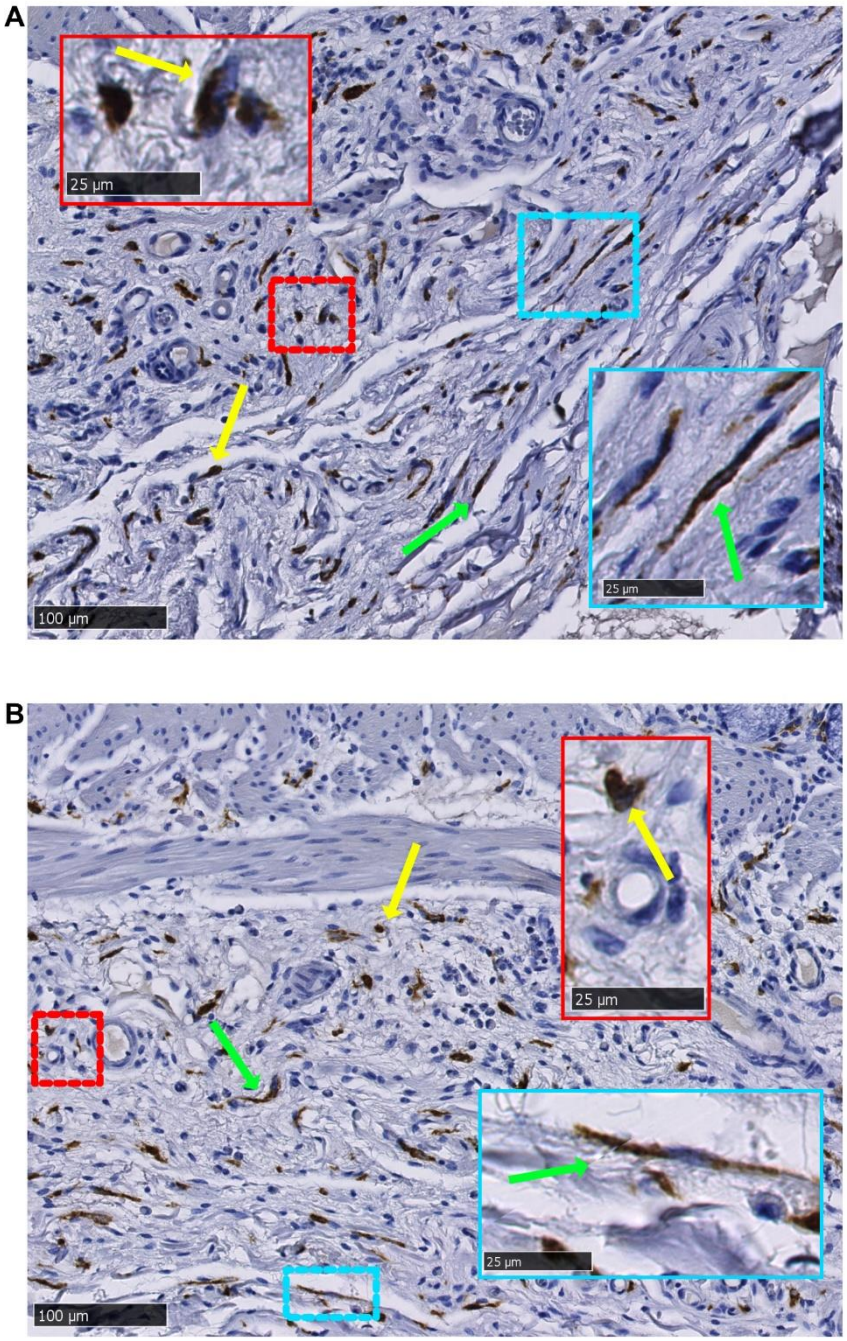

874

875 **Figure 5**

876

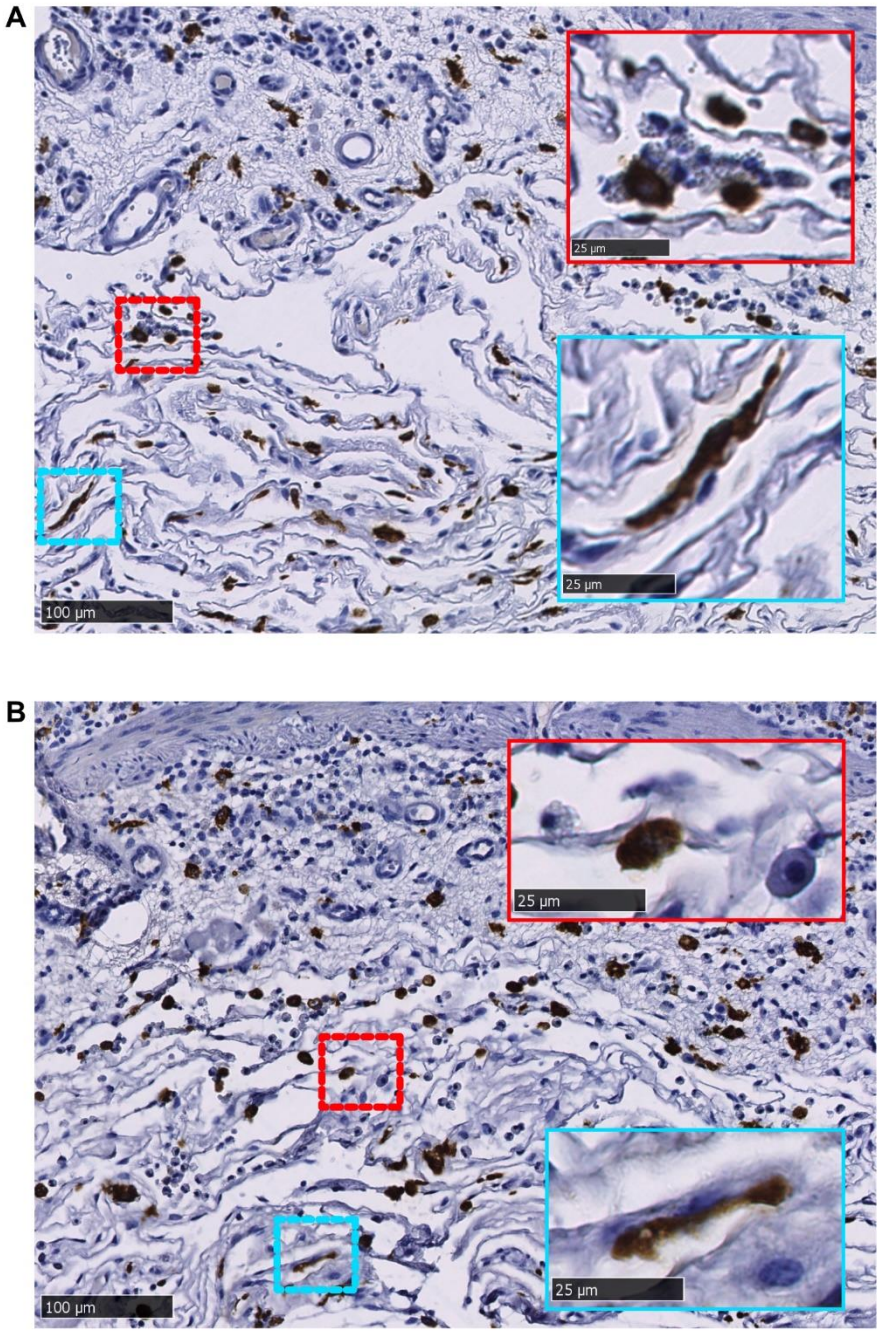

877

878 **Figure 6**

879

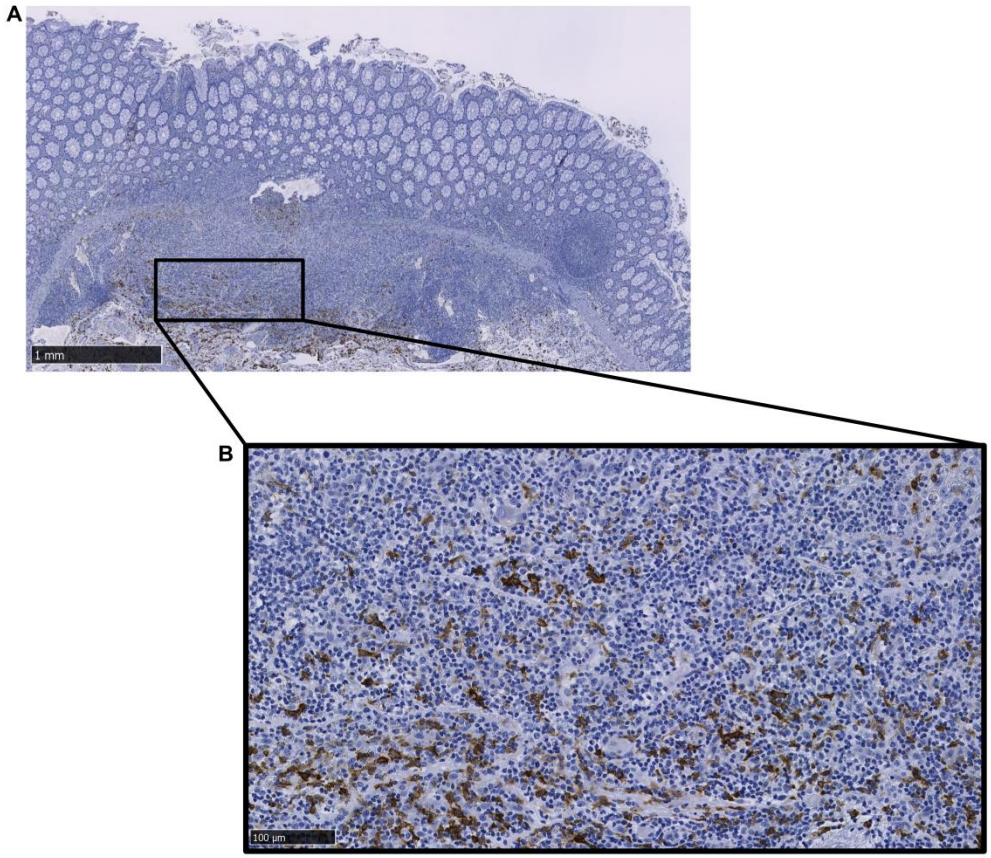

880

881 **Figure 7**

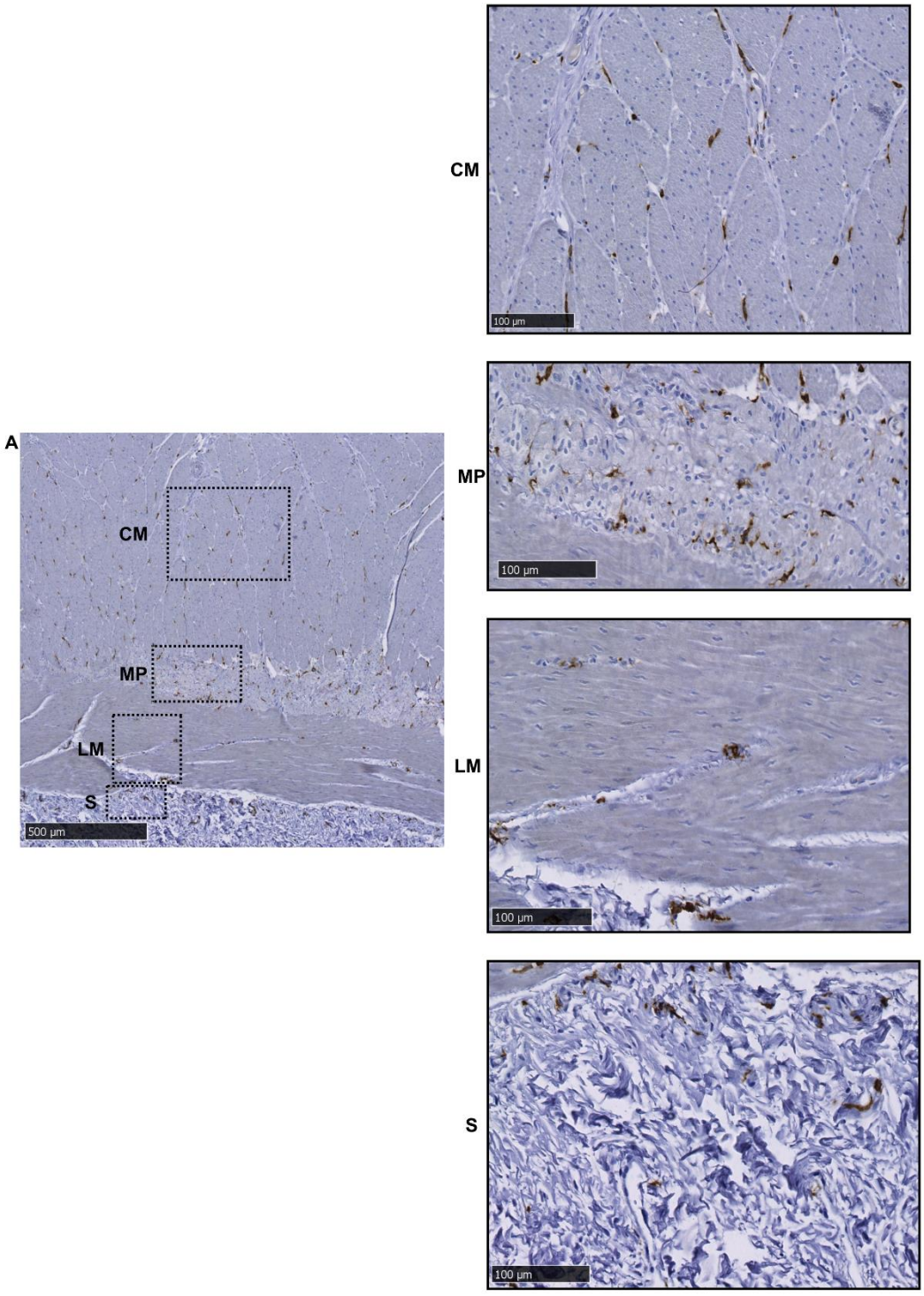

882

883 **Figure 8**

884

885

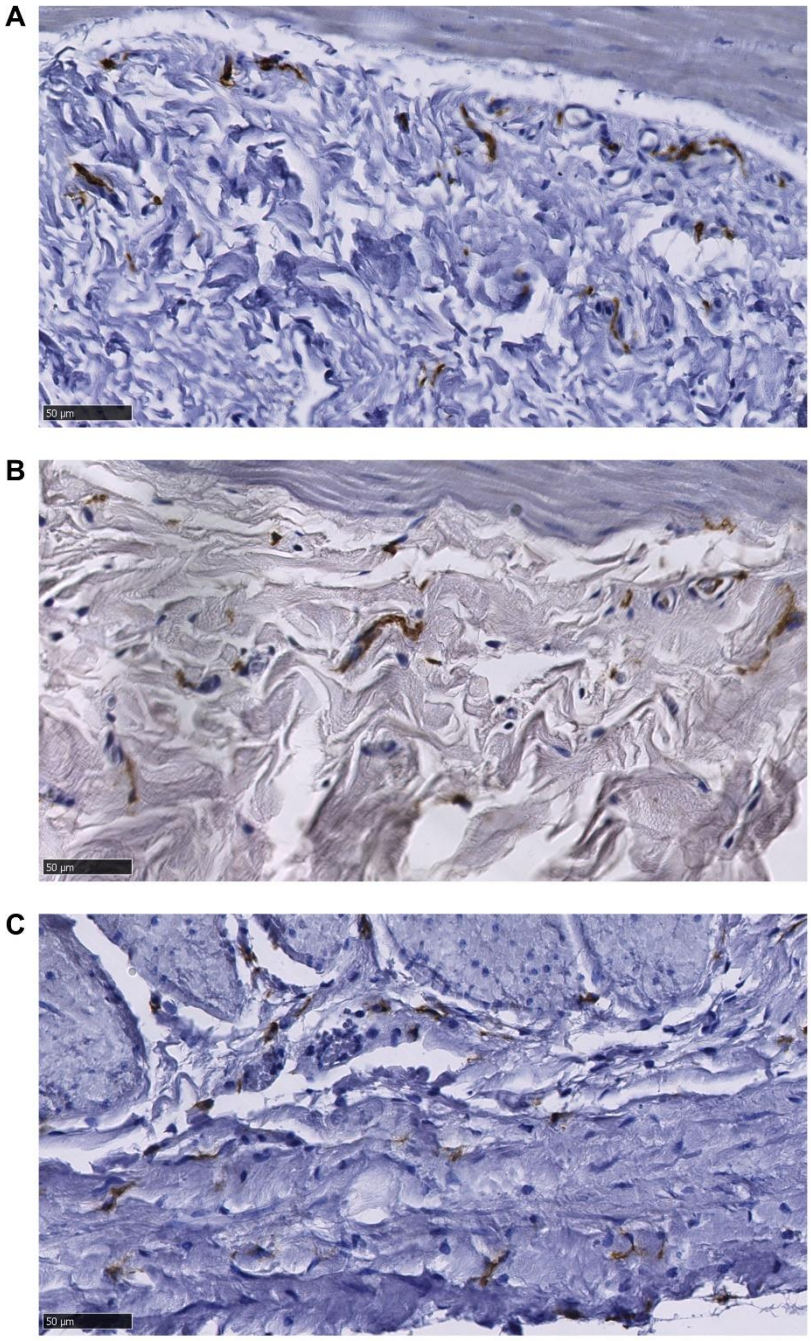

886

887 **Figure 9**

888

889

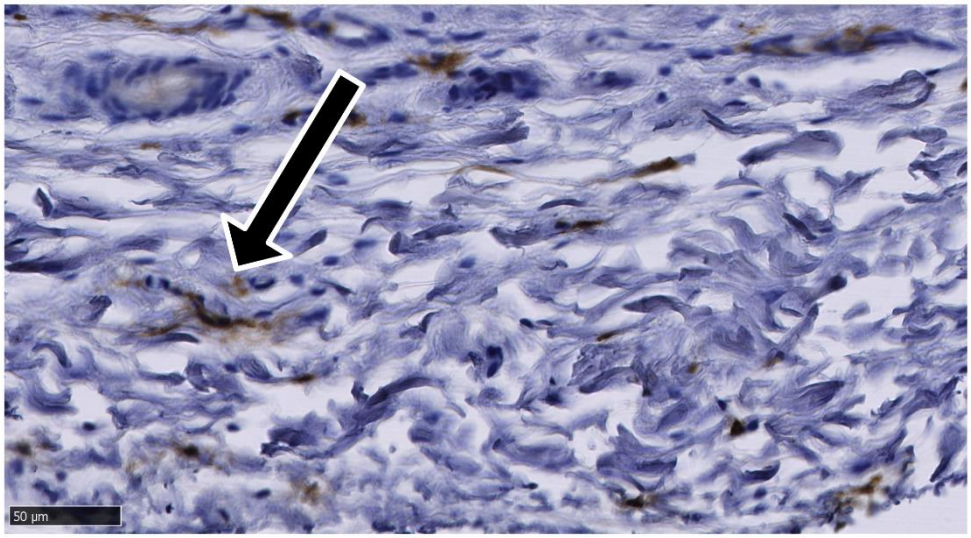

890

891 **Figure 10**

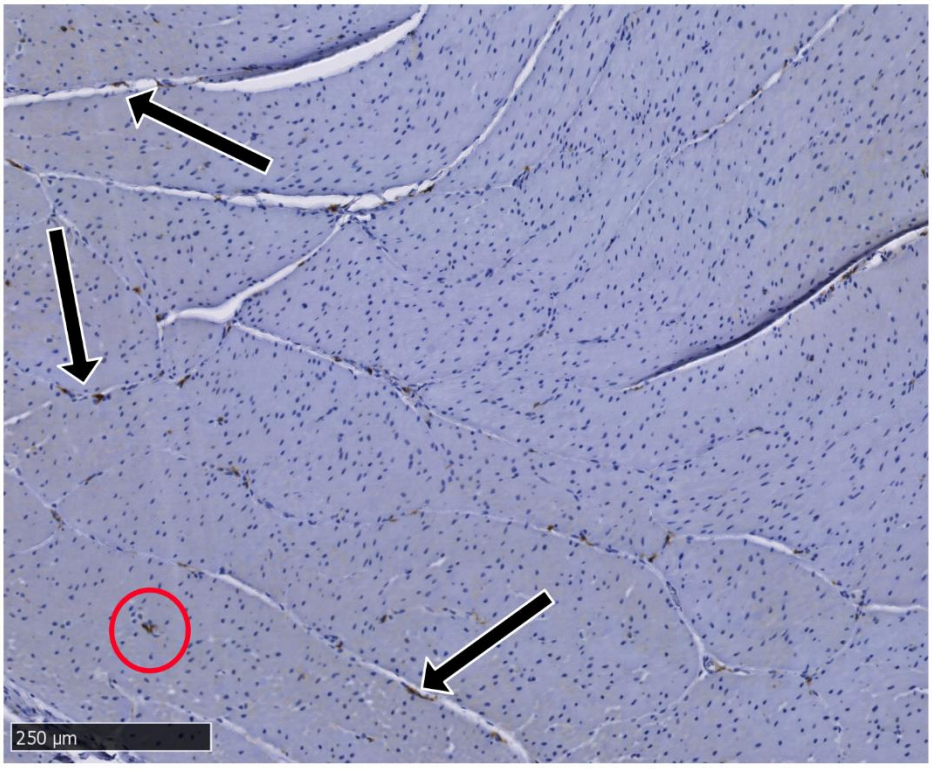

892

893 **Figure 11**

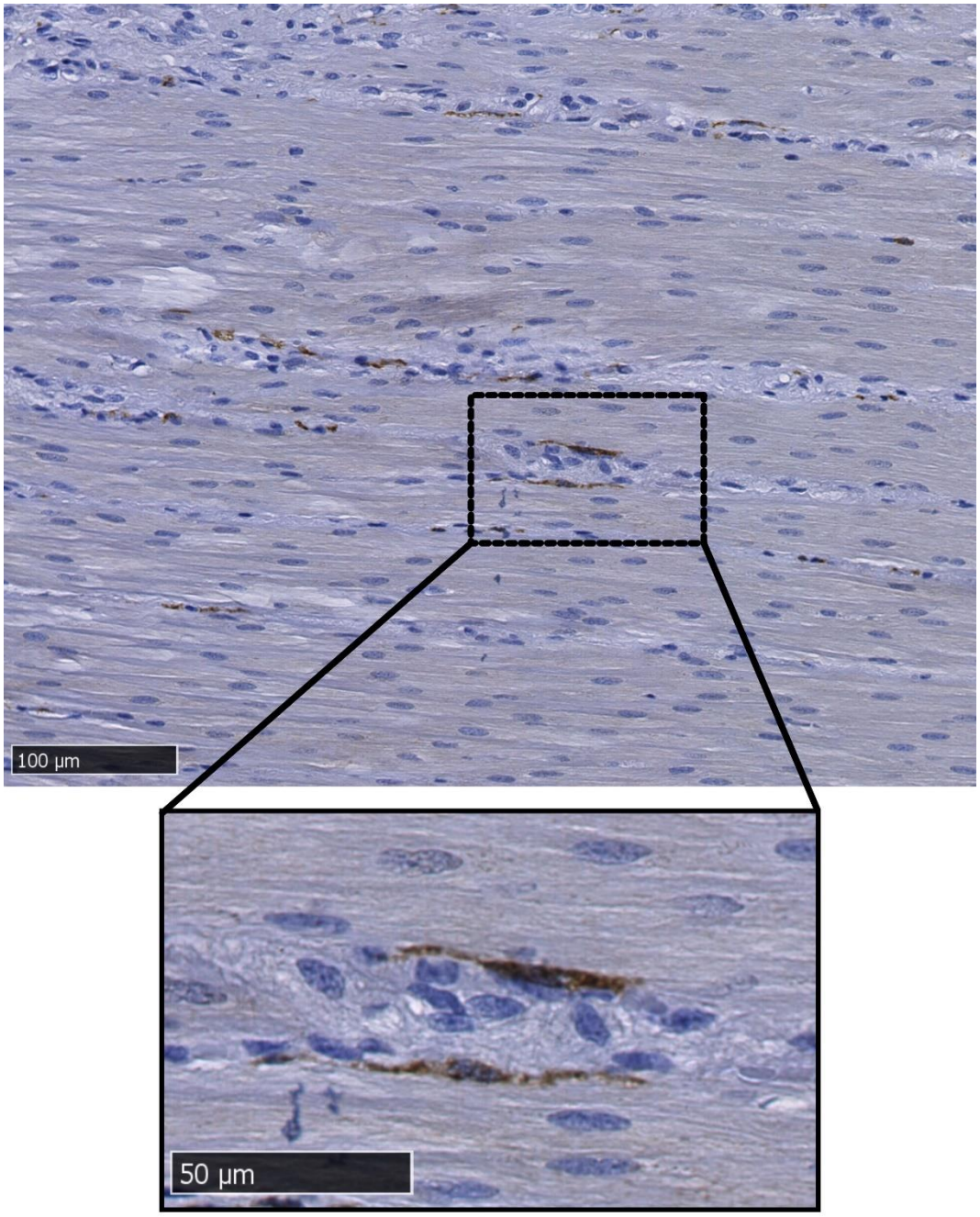

894

895 **Figure 12**

896

897

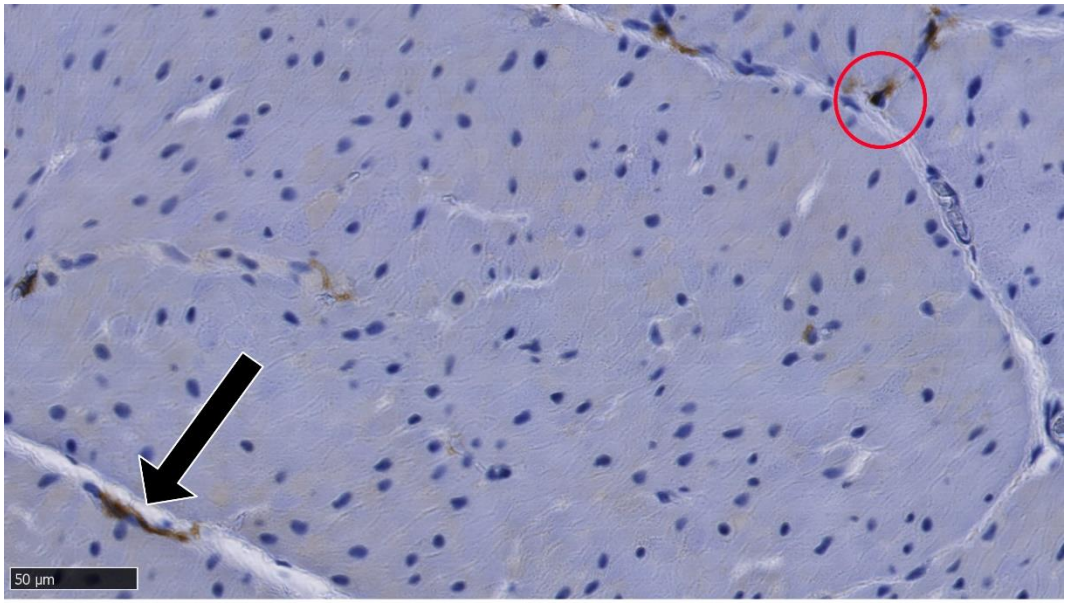

898

899 **Figure 13**

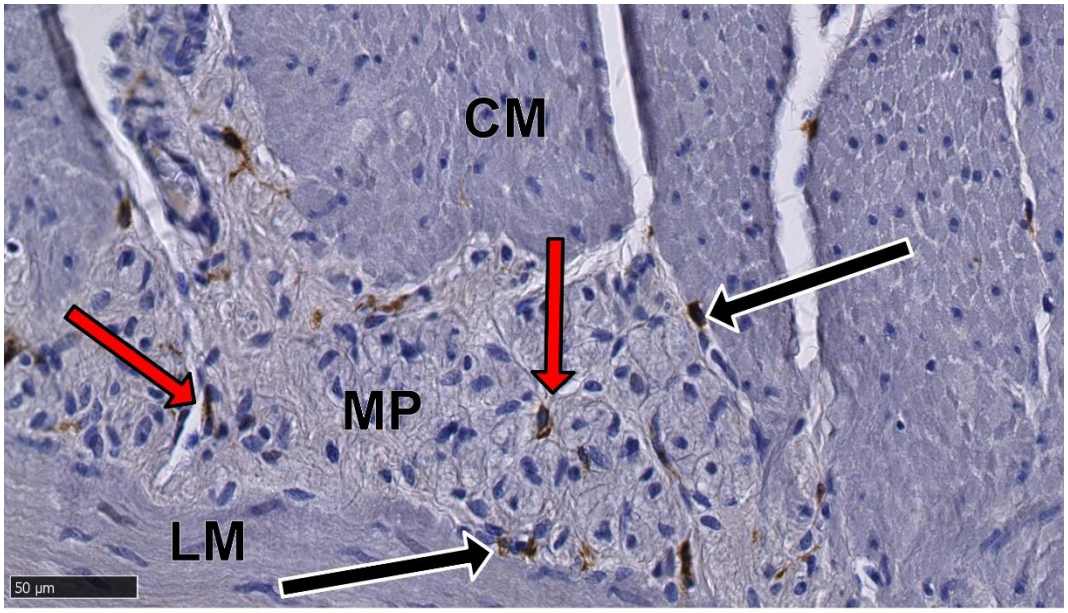

900

901 **Figure 14**

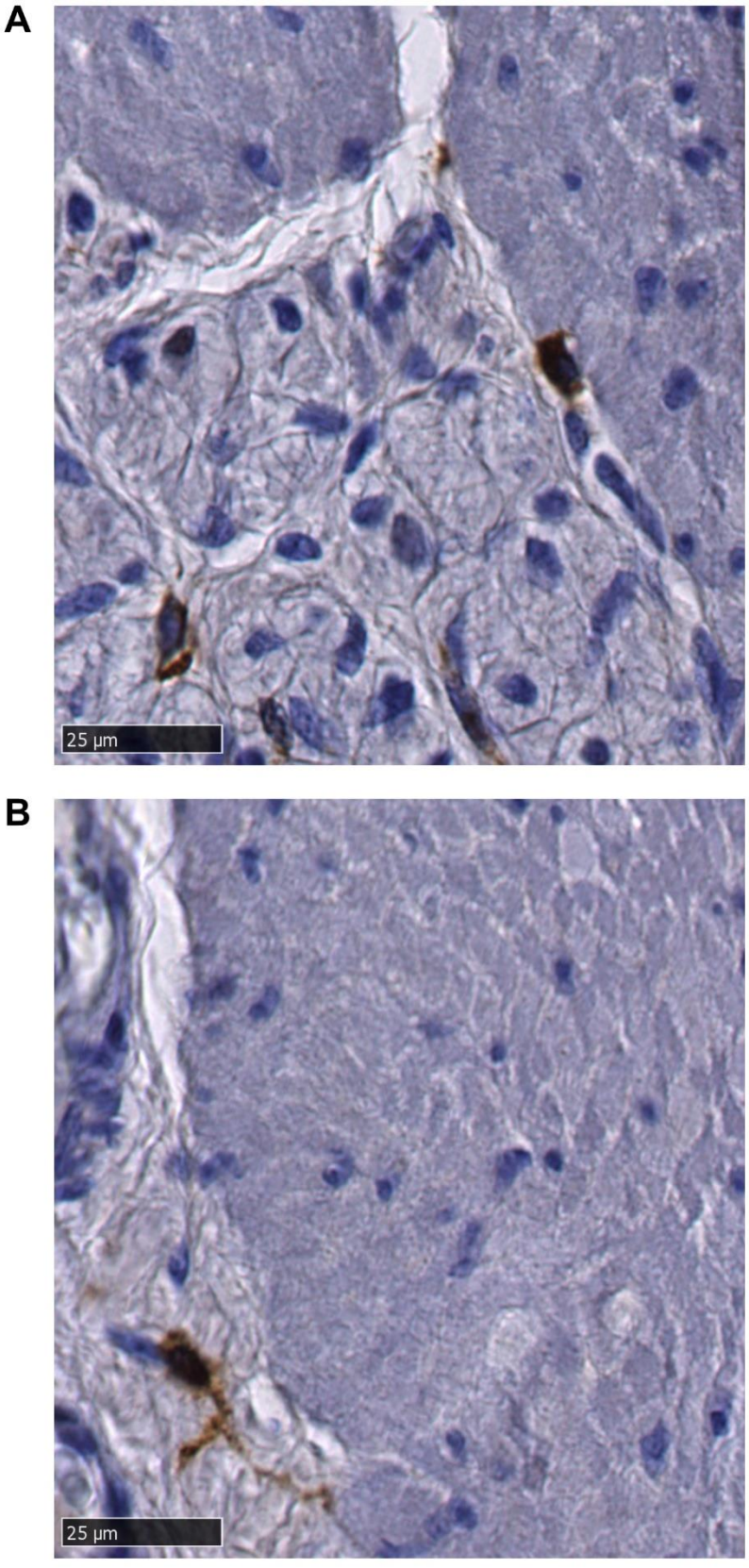

902

903 **Figure 15**

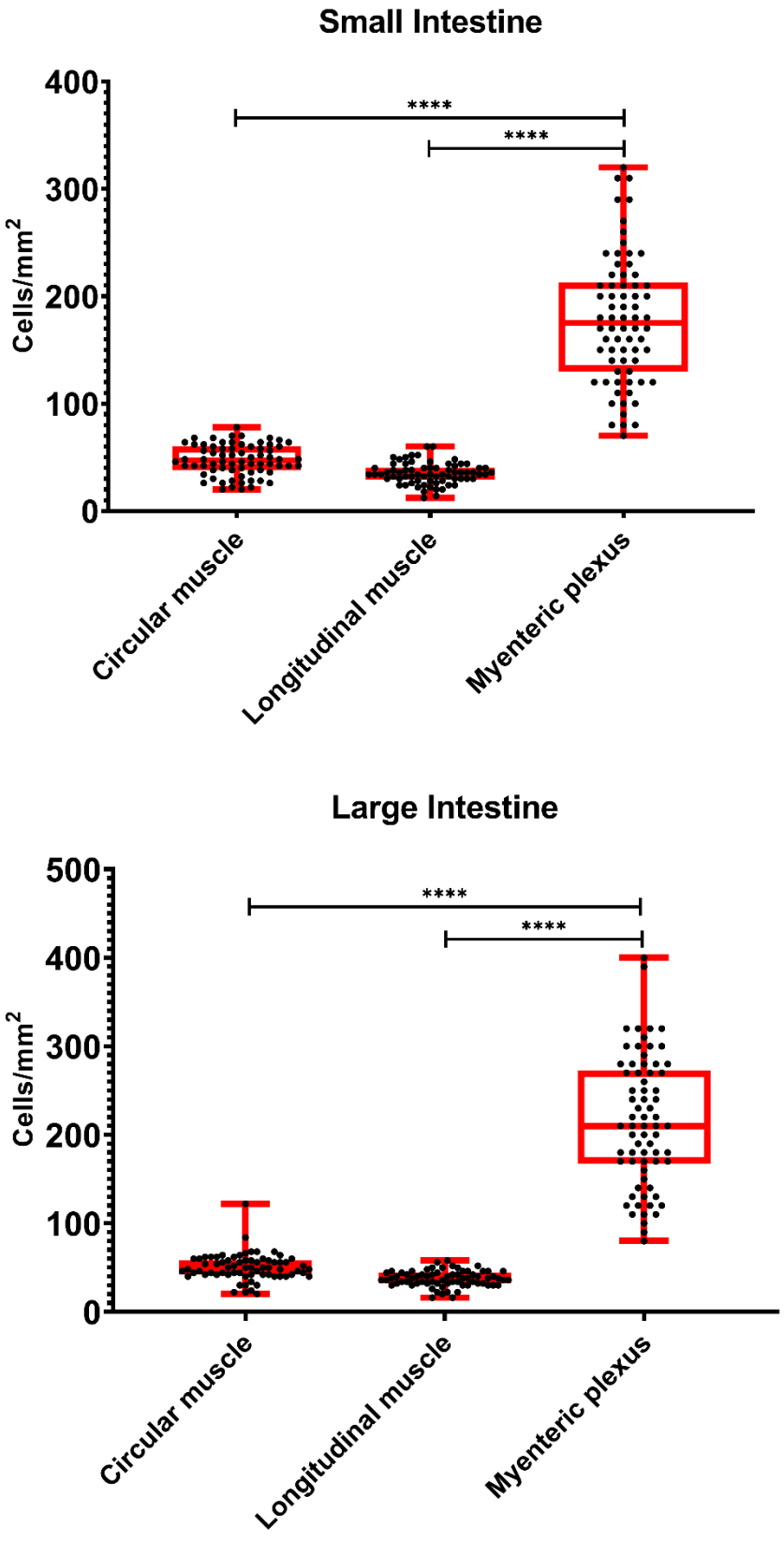

904

905 **Figure 16**